The Implications of Choice between Sour and Sweet Shift on Process Design and Operation of an IGCC Power Plant Integrated with a Dual-Stage Selexol Unit

Elsevier Editorial System(tm) for Energy
Manuscript Draft

Manuscript Number: EGY-D-18-07329R1

Title: The Implications of Choice between Sour and Sweet Shift on Process Design and Operation of an IGCC Power Plant Integrated with a Dual-Stage Selexol Unit

Article Type: Full length article

Keywords: Carbon capture; Selexol; IGCC; Sour shift reaction; Sweet shift reaction; Reactor design

Corresponding Author: Dr. Hyungwoong Ahn,

Corresponding Author's Institution: The University of Edinburgh

First Author: Yixuan Zhang

Order of Authors: Yixuan Zhang; Hyungwoong Ahn

Abstract: In this study, it was sought to design and evaluate two process configurations of an Integrated Gasification Combined Cycle (IGCC) integrated with a dual-stage Selexol unit in which they differ in that one IGCC is configured with sour shift and the other is based on sweet shift. Incorporating water gas shift reactors consuming vast amount of shift steam into an IGCC involves significant alternations to the associated steam cycle, in addition to simply changing the location of the H2S removal step around the shift reactors. It turned out that the sweet shift case would require approximately 4.6 times more shift steam than the sour shift case, as the syngas after H2S removal did not have much steam in it. However, the energy penalties incurred by the carbon capture integration were estimated almost identical regardless of the choice between the sour and sweet shift. This is because the sour shift case would also undergo considerable reduction in power generation at steam cycle due to water quenching. In both shift cases, the high and low temperature shift reactors were sized using the reaction rate models reported in literatures.

Research Data Related to this Submission

There are no linked research data sets for this submission. The following reason is given:
Data will be made available on request

INSTITUTE *for* MATERIALS and PROCESSES

SCHOOL *of* ENGINEERING
The University of Edinburgh
Sanderson Building
The King's Buildings
Mayfield Road
Edinburgh EH9 3JL
Scotland UK

Telephone: +44 (0)131 650 5891
Fax: +44 (0)131 650 6551
Email: H.Ahn@ed.ac.uk

The Editor in Chief
Energy

26th January 2019

TO WHOM IT MAY CONCERN

I am submitting a revised research paper titled 'The Implications of Choice between Sour and Sweet Shift on Process Design and Operation of an IGCC Power Plant Integrated with a Dual-Stage Selexol Unit' to the journal Energy.

This article is partly based on our work presented at the GHGT-14 conference held in Australia. As some of the key outcomes had been publicised to the audience in the conference, I would be very grateful if you could complete reviewing process as quickly as possible.

Please feel free to contact me (Dr. Hyungwoong Ahn, H.Ahn@ed.ac.uk) as a corresponding author if you have any questions or comments relating to this paper submission.

Yours faithfully

Dr Hyungwoong Ahn

Responses to reviewers

Reviewer # 1:

Response: I deeply appreciate your comments. Below are the responses to your comments.

Comment 1: The paper contains the sought to design and evaluate two process configurations of an IGCC integrated with a dual-stage Selexol unit in which they differ in that one IGCC is configured with sour shift and the other is based on sweet shift. The subject and content of this paper complies with the purpose of Energy – the International Journal. There are no Highlights. The Highlights should consists of max. 5 bullet points, each of which should has less than 85 characters according to guideline for Author.

Response: Thanks for pointing out the missing highlights. We formulated the following five highlights to deliver clearly the key messages of this MS.

- Two IGCCs were configured based on sour or sweet shift.
- A dual-stage Selexol process was integrated for capturing CO2.
- Sweet shift case requires 4.6 times more shift steam than sour shift case.
- Energy penalties were almost equal for both sour and sweet shift cases.
- Shift reactors were sized with the catalytic reaction rate models.

Comment 2: The article has 6 keywords. One of them should be changed – "Sour and sweet shift reaction". Keywords can not contain "of" and "and" according to guideline for Authors

Response: Keywords were revised as follows to conform the guideline.

Page 1 (changed): Keywords: Carbon capture; Selexol; IGCC; Sour shift reaction; Sweet shift reaction; Reactor design

Comment 3: The article has no nomenclature. The Authors use a huge number of abbreviations, acronyms and markings. I suggest adding the nomenclature at the beginning of the paper, which will help the reader to decipher individual abbreviations.

Response: In revision, we added nomenclature and abbreviation sections at the beginning of the article as follow:

Nomenclature	
K_e	Equilibrium constant (-)
P	Actual system pressure (atm)
P_i	Partial pressure of component i (kPa)
P_t	Pressure correction factor (atm)
r	Reaction rate ($\mathrm{mol/g_{cat} \cdot s}$)
R	Ideal gas constant ($\mathrm{J/mol \cdot K}$)
T	Temperature (K)
Abbreviation	
BFW	Boiler feed water
COS	Carbonyl sulphide
DS	Dual stage
DOE	Department of Energy
HP	High pressure
HRSG	Heat recovery steam generator
IP	Intermediate pressure
IGCC	Integrated gasification combined cycle
PC-fired	Pulverized coal fired
SSC	Sour shift catalyst

Comment 4: The structure of the paper contains 0 figures, 6 tables and 6 equations. The Authors added 5 figures and 4 tables to supplemental materials.

Response: The original MS contained 6 figures, 6 tables and 6 equations. To address your comments properly, we added one more figure on the hot and cold composite curves of the HRSGs (Figure 6), so now the revision contained 7 figures, 6 tables (+ 7 tables in supplementary materials) and 6 equations.

Comment 5: The literature in paper has 35 references and is appropriately selected. Each has its own reference in the manuscript.
The style of its structure and the way of explaining the methodology and results are good. In particular, the water gas shift reactors section looks interesting. Nevertheless, the paper also has some drawbacks and points to be revised as follows.

Response: We appreciate greatly the reviewer's compliments and criticism. We did our best in correcting the MS to respond properly to the comments. We are confident that the quality of this MS has been greatly enhanced after all the corrections made.

Editorial Remarks

Comment 1: All manuscript; Line numbering on each page does not match the lines of the text and also the lack of numbered pages in manuscript makes the review difficult.

Response: Thanks for your comment. We added the page numbers in the manuscript and we removed the line numbers.

Comment 2: Keywords: One should be changed – "Sour and sweet shift reaction". Keywords can not contain "and" according to guideline for Authors.

Response: The keywords were revised as follow to meet the requirement of guideline.
Page 1: Keywords: Carbon capture; Selexol; IGCC; Sour shift reaction; Sweet shift reaction; Reactor design

Comment 3: Abstract; There is no explanation of the "IGCC" abbreviation in the text of abstract.

Response: The explanation of "IGCC" was added in Abbreviation.

Comment 4: Section 1; There is no explanation of the "PC-fired" abbreviation in the text.

Response: The explanation of "PC-fired" was added in Abbreviation.

Comment 5: Section 1; There is no explanation of the "DOE" abbreviation in the text.

Response: The explanation of "DOE" was added in Abbreviation.

Comment 6: Section 2.1; "given the equilibrium constant, K," or "To achieve the K value", meanwhile in equation (1) is K. Please unify.

Response: We corrected the equilibrium constant as K_e instead of K. Besides, the font of K_e were unified in both text and equations, shown as follow.

Page 6 (changed): K_e

Page 7, equation (1) (changed): $K_e = e^{\frac{4577.8}{T}-4.33}$

Page 7 (changed): K_e

Comment 7: Section 2.1; There is no explanation of the "IP" abbreviation in the text.

Response: The explanation of "IP" was added in Abbreviation.

Comment 8: Section 2.1; There is no explanation of the "BFW" abbreviation in the text.

Response: The explanation of "BFW" was added in Abbreviation.

Comment 9: Section 2.1; There is no explanation of the "HP" abbreviation in the text.

Response: The explanation of "HP" was added in Abbreviation.

Comment 10: Section 2.1; There is no explanation of the "HRSG" abbreviation in the text.

Response: The explanation of "HRSG" was added in Abbreviation.

Comment 11: Section 2.1; There is no explanation of the "DS" abbreviation in the text.

Response: The explanation of "DS" was added in Abbreviation.

Comment 12: All manuscript; The Authors use two ways of writing percentages with values:
first: value % (with space) e.g. (Section 2.1.: "around 10.2 % points" or Section 3.3.: Table 6. 5th row and 3rd, 4th, 5th column – "78.4 %", "77.1 %", "78.5 %" or Section 4: "incur 3.7 %").
second: value% (without space) e.g. (Section 2.1.: "and 4.3% points" or Section 2.2.: "the same 95.5% CO conversion").
Please unify.

Response: Thanks for pointing out this issue. All the percentages with value were unified as the second way, value%, without space.

Page 4 (changed): 0.5%.
Page 8 (changed): 10.2%.
Page 19, Table 6 (changed): 78.4%, 77.1%, 78.5%.
Page 20 (changed): 3.7%.

Comment 13: Section 2.2; There is no explanation of the "COS" abbreviation in the text.

Response: The explanation of "COS" was added in Abbreviation.

Comment 14: Section 3.1; "and 101.32 kPa.." should be "and 101.32 kPa."

Response: The additional full stop has been deleted.
Page 15 (changed): 101.32 kPa.

Comment 15: Section 3.1; "where P is partial pressure [kPa]", meanwhile in equation (2) is P. Please unify.

Response: We corrected the expression of partial pressure as P_i $(i = CO_2, H_2, CO, H_2)$ instead of P. Besides, the font of P_i was unified in both nomenclature and equations. Since P_i has already declared in nomenclature, the explanation of P_i in the text was deleted.
Page 15 (deleted): where P is partial pressure [kPa].
Page 15, equation (2) (changed): $r_{HTC1} = 10^{2.845} e^{\frac{-111000}{RT}} P_{CO} P_{CO_2}^{-0.36} P_{H_2}^{-0.09} \left(1 - \frac{1}{K_e} \frac{P_{CO_2} P_{H_2}}{P_{CO} P_{H_2O}}\right)$

Comment 16: Section 3.1; "as -111kJ/mol" should be "as -111 kJ/mol"

Response: We corrected it in the manuscript.
Page 15 (changed): -111 kJ/mol.

Comment 17: Section 3.1; "where P is partial pressure [Pa]", meanwhile in equation (3) is P. Please unify.

Response: We also corrected the expression of partial pressure as P_i $(i = CO_2, H_2, CO, H_2)$ instead of P here. In equation (3), the partial pressure has the unit of Pa. To unify the unit, equation (3) has changed as below. In addition, the explanation of P_i was also deleted, as it has already shown in nomenclature.

Page 16, equation (3) (changed):

$$r_{LTS} = \frac{6.153 \times 10^{-14} e^{-\frac{3783}{RT}} P_{CO} P_{H_2O} \left(1 - \frac{1}{K_e} \frac{P_{CO_2} P_{H_2}}{P_{CO} P_{H_2O}}\right)}{\left(1 + 1.756 \times 10^{-30} e^{\frac{80410}{RT}} P_{CO} + 9.321 \times 10^{-7} e^{\frac{4109}{RT}} P_{H_2O} + 2.28 \times 10^{-6} e^{\frac{9795}{RT}} P_{CO_2} + 2.739 \times 10^{-15} e^{\frac{83608}{RT}} P_{H_2}\right)^2}$$

Page 16 (deleted): where P is partial pressure [Pa].

Comment 18: Section 3.1; "where P is actual system pressure [atm]", meanwhile in equation (4) is P. Please unify.

Response: As P has already stated in nomenclature, the explanation of P in the text was deleted. In addition, the font of P was also unified in equations and nomenclature.
Page 16 (deleted): where P is actual system pressure [atm].

Comment 19: Section 3.2; There is no explanation of the "SSC" abbreviation in the text.

Response: The explanation of the "SSC" was added in Abbreviation.

Comment 20: Supplementary material: "Figure 2. Steam cycle design: sour shift case." Should be "Figure 3. Steam cycle design: sour shift case".

Response: The figures must have been included in the main text, not in the supplementary materials. And all the figures have been rearranged including the new figure 2.

Comment 21: Supplementary material: Figure 6. (a) – (d); If the values change in the second place after the decimal point, it does not make sense to keep the accuracy to four decimal places.

Response: The figures were generated by UniSim and it was not possible to remove the unnecessary 0 on the graph. Hence, we replotted all the figures in MS-Excel and managed to correct them as follows. Accordingly Table 6 has also been modified.

Table 6 (changed): We presented the reactor volume instead of the reactor length and diameter in this table.

Table 6: Size of the shift reactors estimated by the reaction rate models at the condition of 99% approach to the equilibrium CO conversion.

	Sweet HTSR	**Sweet LTSR**	**Sour HTSR**	**Sour LTSR**
Catalyst	**HTC1 (Fe-based catalyst)**	**LTS (Cu-based catalyst)**	**SSC (CoMo-based catalyst)**	**SSC (CoMo-based catalyst)**
Volume, m^3	84.7	60.6	56.8	615.8
CO conversion rate	77.9%	78.4%	77.1%	78.5%
Average reaction rate, $mol/cm^3/s$	$2.78 \cdot 10^{-5}$	$8.63 \cdot 10^{-6}$	$4.11 \cdot 10^{-5}$	$8.83 \cdot 10^{-7}$

Figure 6 (changed): (renumbered to figure 7).

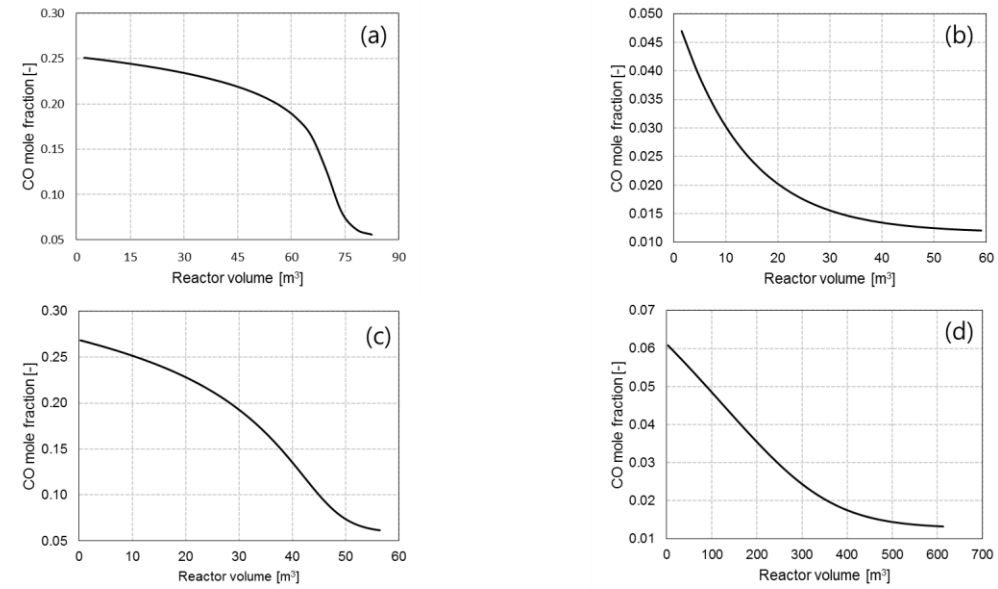

Figure 7. Profiles of CO component mole fractions along the reactor volume: (a) high temperature sweet shift on Fe-based catalysts, (b) low temperature sweet shift on Cu-based catalysts, (c) high temperature sour shift on CoMo-based catalysts, (d) low temperature sour shift on CoMo-based catalysts.

Essential Remarks

Comment 1: In Equation (5) and (6) in Section 3.2, the Authors use "ppm", while in the text Authors use "ppmv". What is the difference between "ppm" and "ppmw"?

Response: When scrutinizing the papers in which the two equations were found, we realised that the H2S concentration must be expressed in ppmv, i.e. $\frac{\text{volume of solute}}{\text{volume of solution}} \times 10^6$. Accordingly, the MS was revised as follows.

Page 16 (changed): 1000 H_2S ppmv

Page 16, equation (5) (changed):

$$r_{SSC,1000ppmv\ H_2S} = 0.008e^{\frac{-60300}{RT}} P_{CO}^{0.75} P_{H_2O}^{0.31} P_{CO_2}^{-0.07} P_{H_2}^{-0.09} \left(1 - \frac{1}{K_e} \frac{P_{CO_2} P_{H_2}}{P_{CO} P_{H_2O}}\right)$$

Page 16 (changed): 330 to 2670 ppmv

Page 16, equation (6) (changed): $r_{SSC} = r_{SSC,1000ppmv\ H_2S} \left[\frac{H_2S\ ppmv}{1000}\right]^n$

Page 17 (changed): 1000 ppmv

Comment 2: With such advanced structures, it is necessary to present detailed assumptions, for example, isentropic and mechanical efficiencies, pinch points and approach points in exchangers, gas turbine operation parameters, compression ratio, COT etc. Without a set of assumptions, the reader is not sure about the results presented.

Response: To address the issues raised, a short summary of the gas turbine was added to the main text, including the firing temperature of the gas combustion chamber, the pressure ratio, the steam cycle pressures, etc. Also we added several tables in supplementary materials to show the approach temperatures of all the heat exchangers (Table S5), the adiabatic and polytropic efficiencies of all the pumps and compressors (Tables S6 and S7), the hot and cold composite curves of the HRSG.

Page 5 (added):

This study is based on two Advanced F class gas turbine to generate 464 MW power in total. The firing temperature of combustion chamber was controlled within the range of 1318-1327°C, with the pressure ratio of 18.5. The net efficiency of such turbines was 57.5% (LHV), giving the net heat rate of 6256 kJ/kWh (LHV). The exhaust gas leaves gas turbine entering the steam cycle via HRSG. The pressure levels for HP/IP/LP sections are 12.5/2.9/0.45 MPa, respectively. In both sour and shift cases, the HRSGs undergo around 533 MW of the heat transfer between the hot and cold streams. The hot and cold composite curves are presented in Figure 2.

Table S5. Approach points of the main heat exchangers.

Heat exchanger	Approach point (°C)	
	Sour	Sweet
High pressure steam generator	29.8	3.5
Raw gas cooler	92.5	66.3
HTSC	19.8	20.8
T-syngas cooler 1	19.4	91.0
T-syngas cooler 2	12.3	-
T-syngas cooler 3	15.9	24.4
T-syngas cooler 4	52.4	60.9
T-syngas cooler 5	9.7	19.7
T-syngas cooler 6	36.7	22.0
Flue gas reheater	116.7	116.7
Lean-solvent cooler	6.7	50.6
Grand Steam Condenser	1.7	1.7
R-syngas cooler 1	-	136.1
Scrubber cooler	4.2	4.2

Table S6: Summary of adiabatic efficiency of pumps.

Pump	Adiabatic efficiency	
	Sour	Sweet
HP pump	70.2%	70.2%
LP pump	80.0%	80.0%
IP pump	81.0%	81.0%
Condensate pump	63.9%	63.9%
H_2S-laden solvent pump	80.0%	75.0%
H_2S concentrator bottom pump	75.0%	-
CO_2-laden solvent pump	80.0%	80.0%
Lean solvent pump	80.0%	80.0%
Semi-lean solvent pump	80.0%	80.0%
Quench water pump	75.0%	-
CO_2 product pump	85.0%	85.0%
Makeup water pump	75.0%	75.0%
Makeup DEPG pump	75.0%	75.0%

Table S7: Summary of adiabatic efficiency and polytropic efficiency of compressors.

Compressor	Sour		Sweet	
	Adiabatic efficiency	Polytropic efficiency	Adiabatic efficiency	Polytropic efficiency
Recycle gas compressor	80.0%	80.4%	-	-

Flash evaporation compressor	80.0%	81.7%	80.0%	81.8%
Sour gas compressor	80.0%	81.0%	80.0%	81.0%
High pressure gas compressor	83.4%	85.0%	83.0%	85.0%
Syngas compressor	-	-	75.0%	75.3%
CO_2 compressor-1	83.1%	85.1%	83.1%	85.0%
CO_2 compressor-2	83.7%	85.0%	83.7%	85.0%
CO_2 compressor-3	83.7%	85.0%	83.7%	85.0%
CO_2 compressor-4	83.6%	85.0%	83.6%	85.0%
CO_2 compressor-5	83.6%	85.0%	83.65	85.0%

Comment 3: I have not found information from the authors about the originality of this article in any section of the paper. What is the novelty presented by the Authors? In the summary, the Authors should emphasize more precisely what the novelty and originality of the article is in comparison with world literature.

Response: The originality and novelty of this MS is two-fold. Firstly, this MS showed that in integrating a dry coal-fed IGCC with a CO2 capture unit the IGCC can be configured based on either sour shift or sweet shift, and the net plant efficiencies of the two shift cases would not be very different from each other. It had been thought, in most papers, that sour shift would be more advantageous than sweet shift in configuring an IGCC with CO2 capture, as a sour shift case requires less steam extraction from the steam cycle than a sweet shift case. This is true, but this benefit is almost completely offset by quenching the syngas with water. Water quenching taken by US DOE design reduces greatly the amount of high pressure steam to be generated.

The second point is that the two shift reactors in series were sized by the catalytic reaction kinetic models reported in open literatures, for both sour and sweet shift cases. There were a few papers in which the shift reactors of the sweet shift case were simulated. But to the best of our knowledge, there has not been a published paper in which the sour shift reactors were sized.

Reviewer #3: The present study the authors have proposed a design of two process configuration of an IGCC integrated with a dual-stage selexol unit.

There are a few points which should be considered for the revision:

Comment 1: The authors should enhance the published articles in this field with more detail.

Response: I believe that the list of references included in the original MS, 35 in total, is quite comprehensive and extensive. In the original MS, the key results of the published articles closely relating to this MS [11,16-20] were summarised well in Table 1, to show the balance of energy of the IGCC designed. If this reviewer had proposed any articles that were deemed relevant but not included in the original MS, we could have added them to the revision.

Comment 2: The authors should present an error analysis for the present method. What are the probable error sources in such 0-D simulation?

Response: All the simulations were constructed with Honeywell UniSim, the commercial chemical flowsheeting programme. The software has been taken by a number of major companies in the field of industrial process design and optimisation, due to its reliability and accuracy evidenced by a number of successful commercial projects. In this respect, we don't think that an error analysis would be deemed necessary. In general an error analysis would be useful in quantifying inaccuracies involved in the course of an experiment, e.g. measurement of temperature, pressure and flowrate or sample analysis. Note that this study was carried out by simulation, not by experiment.

Comment 3: Is it necessary to evaluate the performance of system in off-design situation?

Response: This study was aimed to evaluate and compare the performances of the two IGCC designs based on either sour shift or sweet shift, given the identical heat input to the process. It might be useful to look into how the designed IGCC would behave under various off-design conditions and see if the designed process could cope with such disturbances. But we think that such case studies would be so vast that it has to be covered in a separate paper. Moreover, the steady-state IGCC simulation has to be converted to a dynamic IGCC

simulation, to see the effect of disturbances varying over time on the performance of the designed IGCC. Certainly, such a work is outwith the scope of this work.

Comment 4: The philosophy beyond the used constant? Are they meaningful?

Response: Honestly, it is not clear to us what this reviewer meant by “the used constant”. In this study, we used three constants: equilibrium constant of WGSR reaction, K_e, ideal gas constant, R and rate constants of the catalytic reaction rate equations. It is obvious that the equilibrium constant of WGSR and ideal gas constant cannot be altered. All the rate constants used in this study were taken from the papers published in the reputable journals, so they are deemed accurate.

Comment 5: The design procedure is inherently a multi-objective optimization problem. Considering this issue, the authors should give more detail about economic aspect of their design? Is it feasible? How much is change of maintenance cost and operational cost?

Response: Techno-economic study may be useful in evaluating a process considering both technical and economical aspects. But again it is not within the scope of this work, as this study was aimed to evaluate the two processes that differ in its process configuration in terms of the energy penalty incurred by CO2 capture integration. As for the detailed economic analysis of the IGCCs, please refer to the US DOE study [2007] in the references in which the levelized cost of electricity was reported for various IGCC designs.

The maintenance and operational costs of the two cases investigated would be so close to each other that they could not affect greatly the economics of the IGCCs. The list of equipment contained in the two IGCCs are almost identical to each other, while it is the process configurations that are different between the two. In turn the CAPEX would not change much. The net plant efficiencies of the two IGCCs were almost equal as shown in Table 4, indicating that the OPEXs of the two cases would be close to each other too. Note that the maintenance cost is generally a function of Total Plant Cost (TPC) consisting of maintenance labour and maintenance materials. The TPCs of the two shift cases would be similar to each other, indicating that the maintenance cost would not differ significantly.

***Highlights**

- Two IGCCs were configured based on sour or sweet shift.
- A dual-stage Selexol process was integrated for capturing CO_2.
- Sweet shift case requires 4.6 times more shift steam than sour shift case.
- Energy penalties were almost equal for both sour and sweet shift cases.
- Shift reactors were sized with the catalytic reaction rate models.

The Implications of Choice between Sour and Sweet Shift on Process Design and Operation of an IGCC Power Plant Integrated with a Dual-Stage Selexol Unit

Yixuan Zhang, Hyungwoong Ahn*

School of Engineering, Institute for Materials and Processes,

The University of Edinburgh, Robert Stevenson Road, Edinburgh EH9 3FB, UK

*Corresponding author. Tel.: +44 131 650 5891

E-mail address: H.Ahn@ed.ac.uk

Abstract

In this study, it was sought to design and evaluate two process configurations of an Integrated Gasification Combined Cycle (IGCC) integrated with a dual-stage Selexol unit in which they differ in that one IGCC is configured with sour shift and the other is based on sweet shift. Incorporating water gas shift reactors consuming vast amount of shift steam into an IGCC involves significant alternations to the associated steam cycle, in addition to simply changing the location of the H_2S removal step around the shift reactors. It turned out that the sweet shift case would require approximately 4.6 times more shift steam than the sour shift case, as the syngas after H_2S removal did not have much steam in it. However, the energy penalties incurred by the carbon capture integration were estimated almost identical regardless of the choice between the sour and sweet shift. This is because the sour shift case would also undergo considerable reduction in power generation at steam cycle due to water quenching. In both shift cases, the high and low temperature shift reactors were sized using the reaction rate models reported in literatures.

Keywords: Carbon capture; Selexol; IGCC; Sour shift reaction; Sweet shift reaction; Reactor design

Nomenclature

K_e	Equilibrium constant (-)
P	Actual system pressure (atm)
P_i	Partial pressure of component i (kPa)
P_t	Pressure correction factor (atm)
r	Reaction rate ($\mathrm{mol/g_{cat} \cdot s}$)
R	Ideal gas constant ($\mathrm{J/mol \cdot K}$)
T	Temperature (K)
Abbreviation	
BFW	Boiler feed water
COS	Carbonyl sulphide
DS	Dual stage
DOE	U.S. Department of Energy
HP	High pressure
HRSG	Heat recovery steam generator
IP	Intermediate pressure
IGCC	Integrated gasification combined cycle
PC-fired	Pulverized coal fired
SSC	Sour shift catalyst

1. Introduction

Fossil fuels have long supplied a vast majority of the energy as well as the raw materials our economy needs. With growing concerns with the environmental issues the use of fossil fuels gives rise to, however, it has been sought to replace fossil fuel with renewable resources to enhance sustainability of our society [1]. As various renewable energy technologies have progressed up to commercial stage, it is expected that fossil fuels will lose their position as main energy resources in the future [2]. However, one aspect that fossil fuels cannot be surpassed by renewables easily lingers on. Fossil fuels can produce energy more stably and steadily than renewables, less affected by the weather around the site [3]. Therefore, fossil fuels still play a key role even in the next generation energy mix, supplementing energy production by renewables [2].

As for power generation, coal and natural gas have been the main raw materials among various hydrocarbon fuels [4]. Given the fact that coal reserves are more evenly distributed over the globe than natural gas reserves, use of coal for power generation is expected not to wither in the future even though the plant efficiency of a coal power plant is generally inferior to that of a natural gas combined cycle [5, 6].

However, coals generate the largest CO_2 per unit electricity generated among fossil fuels when combusted for power generation, due to it being characterised by rather large carbon-to-hydrogen ratio [7]. Hence, in the

UK, it has been banned to construct a new coal-based power plant unless its CO_2 emission is to be curtailed significantly by integrating it with carbon capture and storage (CCS) [8]. But CCS is still deemed so expensive that the concept has not been widely materialized into commercialisation yet.

In the chain of CCS, it is known that carbon capture stage accounts for majority of the total energy consumption [9]. Therefore, it is crucial to reduce drastically the energy consumption at carbon capture stage, in order to bring down the overall CCS cost to an affordable level. In this respect, Integrated Gasification Combined Cycle (IGCC) has been considered an attractive alternative to the conventional PC-fired power plant. In IGCC, a pre-combustion capture process can be applied to a synthesis gas (syngas) containing CO_2 at very high pressure. From the thermodynamic point of view, it would be more energy-efficient to separate CO_2 from a high pressure syngas of the IGCC than a low pressure flue gas that a PC-fired power plant emits. In addition, a carbon capture unit can be designed smaller in an IGCC than in a PC-fired power plant, as the high pressure syngas must be smaller in volume than the low pressure flue gas. Accordingly, pre-combustion capture would involve a specific energy consumption less than post-combustion capture. DOE [6] estimated that the cost of electricity (COE) of an IGCC would increase only 35 mills/kWh on average by integrating it with pre-combustion carbon capture, while decarbonising a PC-fired power plant by amine capture would be so expensive that the COE had to increase 49 mills/kWh.

In designing an IGCC integrated with pre-combustion capture, it is essential to include WGSRs (Water-Gas Shift Reactors) to convert CO to CO_2, so that the following CO_2 capture unit can achieve at least 90% capture efficiency. There are largely two different cohorts of shift catalysts available with respect to their resistance to sulphur, that is, sour and sweet shift catalysts. Given the fact the IGCC syngas contains sulphur compounds originating from coals, the syngas has to be cleared of the sulphur species to protect the sweet shift catalysts. As for the choice of sour or sweet shift in decarbonising an IGCC, it was claimed that sweet shift would not be normally taken for coal gasification applications, due to a greater inefficiency arising from having to cool the syngas before the sulphur removal [10]. Most of the past researches on design of an IGCC integrated with pre-combustion capture centred upon sour shift as shown in Table 1. However, there exist a few of works on sweet shift as well, as shown in Table 2 [11-14] .

There have been a few of works carried out to evaluate and compare the sour and sweet shift cases applied to coal gasification for carbon capture. But it appears that the outcomes of the studies are contradictory to each other in contrast to what is expected. Kanniche and Bouallou [15] compared two dry coal IGCC plants integrated with CO_2 capture that were designed based on either sweet or sour shift in terms of net plant efficiency. According to their simulation results, both of the sour and sweet shift cases were estimated to have almost identical net plant efficiencies, with the difference only 0.5% points. Huang et al. [16] compared the sweet and sour shift options applied to the two IGCC reference plants equipped with either GE or Shell gasification. They reported that the sour shift case would be more efficient than the sweet shift case with its net plant efficiency greater by around 1.5% points.

In this study, it was aimed to estimate the energy penalty of an exemplary IGCC plant integrated with either sour or sweet shift, by designing the entire IGCC process based on the DOE study [5]. By doing so, it was possible to identify which alternations to make in designing the pre-combustion capture IGCCs depending on the choice of sweet or sour shift, and quantify the net plant efficiency more accurately. In addition, the sizes of the shift reactors are to be estimated based on the reaction rate models reported in literatures.

Table 1 Summary of energy balances of past researches on pre-combustion capture IGCCs based on sour shift.

Ref.	Cormos et. al.[17]				Descamps et.al. [11]				Cormos et.al. [18]			
Plant performance	IGCC only	IGCC + Capture	Energy change	Energy penalty	IGCC only	IGCC + Capture	Energy change	Energy penalty	IGCC only	IGCC + Capture	Energy change	Energy penalty
Thermal input, MW	1053	1177.7	124.7	-	725.8	847.9	122.1	-	1040.9	1166.9	126	-
Power Summary, MW												
Gas turbine power	334	334	0	3.36%	188.3	211.5	23.2	1.00%	334	334	0	3.46%
Steam turbine power	183.6	200.14	16.54	0.44%	152	135.8	-16.2	4.93%	186.92	197.5	10.58	1.03%
Syngas Expander	1.48	0.78	-0.7	0.07%	24.7	29	4.3	0.02%	0.88	0.78	-0.1	0.02%
Total power generation	519.08	534.92	15.84	3.87%	365	376.3	11.3	5.91%	521.8	532.28	10.48	4.51%
Total auxiliaries	75.18	112.99	37.81	2.45%	49.3	82.9	33.6	2.98%	72.83	111.87	39.04	2.59%
Net power	443.9	421.93	-21.97	6.33%	315.7	293.4	-22.3	8.89%	448.97	420.41	-28.56	7.10%
Net power plant efficiency (LHV)	42.16%	35.83%	-	-	43.50%	34.60%	-	-	43.13%	36.03%	-	-

Ref.	Padurean et al. [19]				Huang et al. [16]				Prins et al. [20]			
Plant performance	IGCC only	IGCC + Capture	Energy change	Energy penalty	IGCC only	IGCC + Capture	Energy change	Energy penalty	IGCC only	IGCC + Capture	Energy change	Energy penalty
Thermal input, MW	1052.9	1177.76	124.86	-	953.3	1066.8	113.5	-	2166.3	2610	443.7	-

Power Summary, MW												
Gas turbine power	334	334	0	3.36%	286	286	0	3.19%	720.6	816.6	96	1.98%
Steam turbine power	184.32	195.24	10.92	0.93%	192.4	175.6	-16.8	3.72%	475.2	525.6	50.4	1.80%
Syngas Expander	1.48	0.55	-0.93	0.09%	0	0	0	0.00%	0	0	0	0.00%
Total power generation	519.8	529.79	9.99	4.39%	478.4	461.6	-16.8	6.91%	1195.8	1342.2	146.4	3.77%
Total auxiliaries	75.08	104.82	29.74	1.77%	61.31	94.01	32.7	2.38%	145.1	259.9	114.8	3.26%
Net power	444.72	424.97	-19.75	6.15%	417.09	367.59	-49.5	9.29%	1050.7	1082.3	31.6	7.03%
Net power plant efficiency (LHV)	42.23%	36.09%	-	-	43.75%	34.46%	-	-	48.50%	41.47%	-	-

Table 2 Summary of energy balance of a pre-combustion capture IGCC based on sweet shift [16].

Plant performance	IGCC only	IGCC + Capture	Energy change	Energy penalty
Thermal input, MW	953.3	1066.8	113.5	-
Power Summary, MW				
Gas turbine power	286	286	0	3.19%
Steam turbine power	192.4	160.9	-31.5	5.10%
Syngas Expander	0	0	0	0.00%
Total power generation	478.4	446.9	-31.5	8.29%
Total auxiliaries	61.31	94.33	33.02	2.41%
Net power	417.09	352.57	-64.52	10.70%
Net power plant efficiency (LHV)	43.75%	33.05%	-	-

2. Process Configuration Studies 2.1. Sour Shift Case

This case was reproduced following the US DOE's work [5] in which the design basis was detailed. In configuring an IGCC, it is essential to select the gas turbine from the beginning. This study is based on two Advanced F class gas turbine to generate 464 MW power in total. The firing temperature of combustion chamber was controlled within the range of 1318-1327°C, with the pressure ratio of 18.5. The net efficiency of such turbines was 57.5% (LHV), giving the net heat rate of 6256 kJ/kWh (LHV). The exhaust gas leaves gas turbine entering the steam cycle via HRSG. The pressure levels for HP/IP/LP sections are 12.5/2.9/0.45 MPa, respectively. In both sour and shift cases, the HRSGs undergo around 533 MW of the heat transfer between the hot and cold streams. The hot and cold composite curves are presented in Figure 2.

By taking shift catalysts of which the activity can be maintained high with the presence of sulphur compound, the shift reactor can process directly the raw syngas containing COS and H_2S without having to pre-treat the syngas but preheating. In integrating the IGCC with pre-combustion capture, it is essential to

have most of the carbon-containing compounds in the feed exist in the form of CO_2, as the ensuing carbon capture unit can separate only CO_2 selectively from the gas mixture. To this end the syngas undergoes water-gas shift reaction which often requires a huge amount of steam as much as approximately 2 moles of H_2O per 1 mole of CO [5]. Also the steam to CO ratio has to be greater than 1.8 to avoid the methanation reaction [21]. It should be noted that the whole process benefits greatly from the fact that the hot syngas already contains a great deal of steam when leaving the water scrubber operating at a high temperature. In this study, the targeted CO conversion rate was set as high as 95.5%, so that the ensuing Selexol process could achieve 90+% carbon capture efficiency easily.

Table 3. Details of the raw syngas flowing into the shift reactor prior to shift steam addition in both sour and sweet shift cases.

	Sour shift case	**Sweet shift case**
Temperature,°C	298	223
Pressure, kPa	3756	3750
Molar flowrate, kmol/s	9.8	5.4
Molar fraction		
CO	0.3096	0.5560
H_2O	0.4784	0.0002
CO_2	0.0114	0.0908
H_2	0.1569	0.2870
N_2	0.0311	0.0562
H_2S	0.0044	trace
Ar	0.0053	0.0095
CH_4	0.0002	0.0004

Given the syngas composition in Table 3, it is possible to estimate the amount of steam that the syngas must contain in order to achieve the CO conversion efficiency of 95.5%, given the equilibrium constant, K_e, defined by [15]:

$$K_e = e^{\frac{4577.8}{T} - 4.33} \quad (1)$$

Assuming the syngas would leave the LTS (Low Temperature Shift) reactor at around 317 °C [5], the equilibrium constant was estimated around 31 by Eq. 1. To achieve the K_e value at 95.5% CO conversion rate, the required amount of steam has to be 6.1 kmol/s, while the flowrate of steam contained in the syngas

is only 4.7 kmol/s. Accordingly, around 1.4 kmol/s of steam has to be sourced and supplemented into the syngas. To this end, the IPBFW is preheated by recovering the heat of the hot raw syngas after HP steam generation (stream 4 in Figure 3). The hot IP BFW is vaporized to IP steam by recovering the exothermic heat of WGSR at the intercooler thereafter. The amount of the IP steam produced in situ is more than enough to provide the additional shift steam required for sour shift. As shown in Figure 4, the IP steam is split into three streams. The second steam is sent to the gasifier at a fixed flowrate and the rest is directed to the HRSG for power generation.

After the syngas is shifted, then it is cooled down to 35 °C at which the dual-stage Selexol process (DS Selexol) operates. In both sour and sweet shift cases, the performance targets that the acid gas removal unit has to achieve were set identically as below.

- 90% carbon capture efficiency
- 99.9+% H_2S recovery
- 98.5+% H_2 recovery
- 97+% CO_2 product purity

The Selexol solvent can absorb H_2S more strongly than CO_2 with the selectivity of H_2S over CO_2 around 9 [22]. As shown in Figure 3, firstly the syngas enters the H_2S absorber where its H_2S is absorbed by the CO_2-laden solvent originating from the CO_2 absorber. The H_2S-laden solvent leaving the absorber contains significant amount of CO_2 as well as H_2S. The CO_2 has to be stripped off the solvent before the solvent is regenerated thermally in the ensuing steam stripper. Otherwise, the sour gas would end up with containing vast amount of CO_2 as well as H_2S, making it very hard to achieve the stringent target of the carbon capture efficiency. To this end, removing the CO_2 from the solvent were carried out by a H_2S concentrator (gas stripping) followed by a flash evaporation (depressurisation). By doing so it was possible to direct most of the CO_2 contained in the solvent to the CO_2 absorber, facilitating such a high carbon capture efficiency.

In the CO_2 absorber, the CO_2 in the feed is selectively absorbed by two solvent streams: one solvent is the lean solvent generated at the steam stripper, containing effectively no CO_2 in it, and the other is the semi-lean

solvent originating from the flash drums, less regenerated than the lean solvent. As studied previously by the author [23-25], it is crucial to increase the flowrate of the lean solvent flowrate rather than the semi-lean solvent, if such a high carbon capture efficiency as 95% is targeted (high lean case). But there exists a maximum flowrate that the lean solvent cannot exceed. If too much CO_2-laden solvent was sent to the H_2S absorber, then it would not be possible to recover sufficient CO_2 and return it to the CO_2 cycle. Meanwhile, it is also possible to reach the 90% carbon capture efficiency by increasing the semi-lean solvent, without having to increase the lean solvent (low lean case). In other words, the minimum flowrate of the CO_2-laden solvent required to remove 99.9+% H_2S is found and the stream becomes the lean solvent after being regenerated thermally. In low lean case, the total flowrate of the circulating Selexol solvent would be larger, but it would be easier to return the CO_2 carried by the CO_2-laden solvent to the CO_2 removal section. The total energy consumptions of the two cases were estimated similar to each other.

The net plant efficiency of the IGCC integrated with DS Selexol and sour shift was estimated by process simulation using Honeywell UniSim. As shown in Table 4, the energy penalty incurred by carbon capture integration was around 10.2% points. The energy penalties at the steam turbine and the auxiliaries were 4.6 and 4.3% points, respectively (Table 5). It should be noted that the increase of the power consumption at the auxiliaries were mainly due to addition of CO_2 capture and compression. The reduction in the steam turbine power generation by carbon capture integration was mainly due to great difference of the amounts of HP steam generated at the syngas cooling stage immediately after the gasifier. In the sour shift case, it is crucial to have the raw syngas contain a vast amount of steam, so that the ensuing sour shift reactors do not require additional shift steam much. To this end, quenching the raw syngas by adding the water is followed by the syngas cooler and the syngas scrubber operating deliberately at a high temperature (200 °C), compared to 110 °C in the non-capture case. The higher temperature does the syngas scrubber operate at, the more steam the syngas can contain [26]. After the syngas quenching, the syngas temperature falls down to 408 °C, so the amount of the HP steam to be generated by syngas cooler is very limited.

Table 4. Plant performances of decarbonised IGCCs and their comparison with the reference studies.

		Non capture (DOE case 5 [5])	Sour shift (DOE case 6 [5])	Sour shift (This study)	Sweet shift (This study)
Thermal input, MW (HHV)		1547.5	1617.8	1617.8	1617.8
WGSR CO conversion		-	95.6%	95.5%	95.5%
H_2 recovery at DS Selexol		Not reported	Not reported	98.8%	98.5%
H_2S recovery		99.5%	99.7%	99.9+%	99.9+%
CO_2 capture efficiency at the CO_2 absorber		-	Not reported	96.7%	96.2%
Overall carbon capture rate		-	90.0%	89.9%	90.0%
Steam-to-CO ratio		-	2.00	2.03	2.16
Power					
ST power, MW	HP turbine	-	-	44.5	61.2
	IP turbine	-	-	73.6	64.1
	LP turbine	-	-	104.9	94.7
	Total	284.0	229.9	222.9	220.0
GT power, MW		464.0	464.0	464.0	464.0
Total power generation, MW		748.0	693.9	686.9	684.0
AGR auxiliaries, MW		-	15.5	21.6	18.6
Other auxiliary		112.2	132.9	132.8	132.1
CO_2 Compression, MW		-	28.1	32.9	34.4
Total auxiliary power, MW		112.2	176.4	187.4	185.1
Net power, MW		635.8	517.1	499.5	500.9
Net plant efficiency		41.1%	32.0%	30.9%	31.0%

Table 5. Plant performances of decarbonised IGCCs based on sour and shift in this study.

Plant performance	**Non-capture case (DOE case 5, [5])**	**Sweet shift**			**Sour shift**		
		Performance	Energy change	Energy penalty	Performance	Energy change	Energy penalty
Thermal input, MW	1547.5	1617.8	70.3	-	1617.8	70.3	-
Gas turbine power	464.0	464.0	0.0	1.30%	464.0	0.0	1.30%
Steam turbine power	284.0	222.0	-62.0	4.63%	222.9	-61.1	4.57%
Total auxiliaries	112.2	185.1	72.9	4.20%	187.4	75.3	4.34%
Net power	635.8	500.9	-136.9	10.10%	499.5	-136.3	10.20%
Net power plant efficiency (HHV)	41.1%	31.0%	-	-	30.9%	-	-

2.2. Sweet Shift Case

In this case, sweet catalysts replaced the sour catalysts, which requires rearrangement of the DS Selexol unit and shift reactors so that shift reactors are to be placed in between desulphurisation and CO_2 removal as shown in Figure 5. However, this seemingly simple change also requires other units to be modified.

It should be noted that, in sweet shift case, the raw syngas does not have to contain vast steam nor maintained hot after the syngas scrubber [26], as this syngas will be sent to the low-temperature H_2S absorber in prior to shift reactors. The syngas does have to contain some water for COS hydrolysis, but the required amount of steam must be very small taking into account the tiny amount of COS in it. In this respect, quenching is no longer needed and the process configuration around the gasifier reverts to what was originally designed for the non-capture case in which it was aimed to generate as much HP steam as possible by heat recovery. The syngas cooling section consists of two heat exchangers for HP steam generation followed by IP BFW heating as is in the sour shift case. The heat duty available in the syngas cooling was distributed over the two heat exchangers by estimating the heat duty at the IP BFW preheater first. The flowrate of the IP BFW to be preheated can be determined by the amount of heat available at the intercooler of the shift reactors in which the IP BFW is to be boiled.

After syngas scrubbing, the syngas is slightly heated by hot HP BFW and then fed to COS hydrolysis in the same way as the syngas is processed in the non-capture case. Then the syngas is cooled down to 35 °C at which the H_2S absorber operates. In the H_2S absorber, the H_2S of the syngas is absorbed selectively by the Selexol solvent originating from the CO_2 absorber. However, the syngas in sweet shift case is very different from that in sour shift case with respect to the composition. In sour shift case, the syngas contains a great amount of CO_2 (45 vol.%) as a result of shift reaction. On the contrary, the syngas in the sweet shift case contains a relatively low amount of CO_2 (3 vol.%). Accordingly, when the CO_2-deficient syngas contacts the CO_2-laden solvent in the H_2S absorber, the CO_2 dissolved in the solvent is stripped off by the syngas. In other words, the H_2S absorber works to absorb the H_2S from the syngas and at the same time strip the CO_2 off the solvent, transferring significant amount of CO_2 from the solvent to the syngas. In turn, it is possible to restrict the CO_2 slip into the sour gas, without having to have a separate H_2S concentrator. Hence, the sweet shift case does not have a H_2S concentrator as shown in Figure 5.

However, the augmented amount of CO_2 in the syngas stream after H_2S removal affects adversely the ensuing shift reaction with respect to the reaction equilibrium. After the gas feed picks up CO_2 upstream of the WGSR, it becomes harder to achieve the targeted CO conversion rate. The greater amount of CO_2 the

syngas contains, the more shift steam has to be added to achieve the targeted CO conversion rate. In addition, the syngas leaving the H_2S absorber is still at low temperature, containing much less water vapour than the syngas feed flowing into the sour shift reactor in which it contains significant amount of steam as shown in Table 1.

The amount of CO_2 being transferred from the CO_2-laden solvent to the syngas in the H_2S absorber is highly affected by the flowrate of the CO_2-laden solvent to the H_2S absorber. Increasing the solvent flowrate around the H_2S cycle would make it easier to achieve a very high CO_2 capture rate, as the pinch point is to be formed around the top of the CO_2 absorber to which the CO_2-free Selexol is admitted [25].

The targeted carbon capture efficiency of 90% could be achieved by changing the ratio of the flowrate of the CO_2-free solvent originating from the steam stripper to the flowrate of the semi-lean solvent from the flash drums. As explained above, increasing the CO_2-free solvent flowrate would facilitate reaching the 90% of carbon capture efficiency, as the solvent admitted to the absorber on the top is capable of absorbing CO_2 more strongly than the semi-lean solvent entering the column in the middle. To do so, the flowrate of the CO_2-laden solvent flowing from the CO_2 absorber to the H_2S absorber has to be increased. In turn, it is inevitable to see the syngas pick up more CO_2 from the solvent in the H_2S absorber with the increasing CO_2-laden solvent flowrate. More shift steam would have to be added to the syngas to achieve the targeted CO conversion rate. As discussed in [21], WGSRs often accounts for the largest energy penalty in integrating IGCC with carbon capture. In this respect, it is crucial to maintain the usage of shift steam as low as possible in order to bring down the energy penalty in overall. As a result, low lean case was chosen so as to minimise the flowrate of the CO_2-laden solvent to the H_2S absorber (low lean case).

Assuming the same equilibrium constant of 31 at the outlet of the LT shift reactor, it is also possible to estimate the steam flowrate required to achieve the same 95.5% CO conversion rate by mass balance. When leaving the H_2S absorber, the syngas contains negligible amount of water vapour at 0.0008 kmol/s, while the required total steam flowrate amounts to 6.5 kmol/s, 0.4 kmol/s greater than the flowrate in sour shift case due to the sweet syngas containing more CO_2 than the syngas in the sour shift case. Therefore, a vast amount of steam has to be added to the syngas.

To source the shift steam, several changes were made to the sour shift case. In sour shift case, the IP steam generated by heat recovery at the intercooler between two shift reactors is split into three sub-streams as shown in Figure 4. The first two streams are used as the diluent of the gasifier and the shift stream. And the rest of it is sent to the HRSG where it is superheated for power generation. In sweet shift case, the portion of the shift steam has to be maximised to compensate the greater demand for shift steam, indicating that no steam is available for power generation any more (Figure 6).

But the increment of the shift steam flowrate is still not large enough for the targeted CO conversion rate. Therefore, another source of shift steam had to be found in the steam cycle. In this study, the additional shift steam was extracted from the HP turbine exhaust. To this end the back pressure of the HP turbine had to be increased up to 38.0 bar from 31.1 bar as the syngas feed has to enter the HT shift reactor at 37.6 bar. The pressure change made to the HP turbine results in significant reduction in the power generation at the HP turbine.

Once shifted, the hot syngas leaving the low temperature shift reactor is cooled down to 35 °C to feed it to the CO_2 absorber. At the same time, the heat is recovered to preheat the WGS feed gas and quenching water and also generate LP steam. It is noticeable that the syngas after sweet shift contains more CO_2 (3.39 kmol/s) and steam (3.63 kmol/s) than the syngas in sour shift case does (3.00 kmol/s CO_2 and 3.26 kmol/s steam), resulting in the total syngas flowrate being larger in sweet shift case (12.0 kmol/s) than in sour shift case (11.3 kmol/s). This is because the syngas feed to shift reaction contains more CO_2 in sweet shift case (0.494 kmol/s) than in sour shift case (0.112 kmol/s) on the grounds of some CO_2 being added to the syngas in the H_2S absorber in the sweet shift case, and accordingly more excess steam has to be added to the syngas for achieving the CO conversion rate. As the shifted syngas has a greater flowrate in sweet shift case, carrying greater heat, its heat recovery can generate more LP steam.

The cold shifted syngas after heat recovery is returned to the DS Selexol unit for carbon capture. Once processed in DS Selexol unit, the treated syngas stream entering the gas cycle are almost identical in both shift cases in terms of the flowrate and gas composition, indicating that the power generation at the gas cycle would also be identical.

However, the power generation at steam cycle could not but differ significantly between the two cases. Compared to the sour shift case, the sweet shift case has to undergo the following alternations to its steam cycle. The alterations resulting in reduction of the power generation are:

- Reduction of the back pressure of the HP turbine.
- Extraction of the HP turbine exhaust for shift reaction.
- Directing the IP steam generated by recovering the exothermic shift heat to the WGSR instead of the steam cycle.

On the contrary, the changes leading to increase of the power generation are:

- Generating a far greater amount of HP steam at the syngas cooling stage, as quenching is not needed.
- The amount of LP steam generated by cooling the shifted syngas increases, as the syngas is at a higher flowrate, containing more CO_2 and steam.
- Extraction of part of the HP turbine exhaust for shift steam results in less reheat duty in HRSG. Accordingly the HP BFW flowrate admitted to the HRSG is to be increased.

In overall, the amounts of power generation in both sour and sweet shift cases are almost equal, while the power generations at individual steam turbines are very different from each other. The differences between the two shift cases can be explained qualitatively as follows.

- The sweet shift case can generate the HP steam far greater than the sour shift case, resulting in greater power generation at HP turbine. The positive effect of more HP steam generated at syngas cooling outweighs the negative effect of the back pressure of the HP turbine increasing.
- The shift reactors of the sweet shift case require a far greater amount of additional IP steam. Accordingly, the power generation at the IP turbine is reduced significantly due to a huge amount of IP steam being extracted from the steam cycle.
- The difference of the power generations at the LP turbine in two shift cases is similar to that at the IP

turbine, in spite of the amount of LP steam generated by cooling the shifted syngas being slightly greater in sweet shift case. This is because the LP steam from shifted syngas cooling is of lower quality than the HRSG LP steam with respect to the temperature.

3. Water Gas Shift Reactors

In this section, it was aimed to estimate roughly the size of the two shift reactors in each shift case based on the reaction rate models reported in open literatures. The syngas undergoes water gas shift reaction at two reactors in series: a high temperature shift reactor (HTSR) followed by a low temperature shift reactor (LTSR). The HTSR converts bulk CO to CO_2, while the LTSR can reduce the CO content less than 2 vol.% on dry gas basis.

In the shift reactors, there are several side reactions other than the main reaction taking place at the same time, such as COS hydrolysis, Fischer-Tropsch synthesis, methanol synthesis, etc. But these minor reactions were disregarded in this study, assuming that incorporating these reactions into the reactor models would not affect much the estimation of the reactor size.

All the shift reactors were simulated by a Plug Flow Reactor (PFR) module available in Honeywell UniSim that allows to simulate various heterogeneous catalytic reaction rate models. The overall CO conversion rates in the two shift cases were identical around 95.6%. Due to the high moisture content in the syngas leaving the scrubber, the sour shift needs less steam-to-CO ratio than the syngas in sweet shift case. It was estimated that the ratio of steam to CO was 2.16 in sweet shift and 2.03 in sour shift.

3.1. Sweet Shift

Fe- and Cu-based catalysts were taken for HTSR and LTSR, respectively. As for the high-temperature shift catalyst, the reaction rates were estimated by a power-law rate model [27]. In the Hla et al.'s study [27], two different Fe-based shift catalysts (HTC1 and HTC2), differing with respect to its constituent compositions,

were tested and the reaction kinetic models were constructed based on the experimental data. As a result, HTC1 was chosen in this study on the grounds that HTC1 would perform better than HTC2 for a feed gas containing high CO and low CO_2 and H_2, as with the syngas in this study.

Hla et al. [27] proposed the parameter values of the power-law model by testing the HTC1 (80-90 wt% Fe_2O_3/8-13 wt% Cr_2O_3/1-2 wt% CuO) with sulphur-free syngas at 360 – 450 °C and 101.32 kPa.

$$r_{HTC1} = 10^{2.845} e^{\frac{-111000}{RT}} P_{CO} P_{CO_2}^{-0.36} P_{H_2}^{-0.09} \left(1 - \frac{1}{K_e} \frac{P_{CO_2} P_{H_2}}{P_{CO} P_{H_2O}}\right) \quad (2)$$

The raw syngas undergoes the CO conversion rate of around 79% in the HTSR. The hot syngas leaving the HTSR is cooled by boiling hot IP BFW and then it is fed successively to the ensuing LTSR for reducing the CO mole fraction further.

As can be seen in the reaction kinetic model of the HTC1, the activation energy of the rate constant is as high as -111 kJ/mol, indicating that the reaction rate would be very low in the temperature range of the LTSR, 270 – 317 °C. In this relatively low temperature range of the LTSR, the Fe-based HTS catalyst would end up with a very low reaction rate.

Hence a Cu-based catalyst, exhibiting a very high reaction rate in the low temperature, has to be chosen instead. In this study, it was assumed that the LTSR was packed with a commercial CuO/ZnO/Al_2O_3 (50/40/10 wt%) catalyst referred to LTS. Mendes et al. [28] proposed a Langmuir-Hinshelwood model along with its associated parameter values by testing the Cu-based catalyst with sulphur-free syngas in the range of 180 – 300 °C and at 101.32 kPa as follows [28].

$$r_{LTS} = \frac{6.153 \times 10^{-14} e^{-\frac{3783}{RT}} P_{CO} P_{H_{2O}} \left(1 - \frac{1}{K_e} \frac{P_{CO_2} P_{H_2}}{P_{CO} P_{H_2O}}\right)}{\left(1 + 1.756 \times 10^{-30} e^{\frac{80410}{RT}} P_{CO} + 9.321 \times 10^{-7} e^{\frac{4109}{RT}} P_{H_{2O}} + 2.28 \times 10^{-6} e^{\frac{9795}{RT}} P_{CO_2} + 2.739 \times 10^{-15} e^{\frac{83608}{RT}} P_{H_2}\right)^2} \quad (3)$$

According to Eq.3, the Cu-based catalyst would have a reaction rate greater than the Fe-based catalyst, even at the operation conditions of the HTSR. However, the Cu-based catalyst had to be employed for a shift

reactor operating in the relatively low temperatures, as it would be easily deactivated by thermal sintering in the HTSR temperature [29].

In estimating the reaction rates at the IGCC pressure as high as 35 bar, it may be presumptuous to make use of the reaction rate models constructed by testing the catalysts at ambient pressure. In this respect, Eq. 4 was taken as a pressure correction factor and is applied to each reaction rate model, similarly to the earlier works [30, 31].

$$P_t = P^{0.5-P/500} \quad (4)$$

The pressure correction factor is known to be valid up to 55 atm [32, 33].

3.2. Sour Shift

It is not recommended to use the sweet shift catalysts presented above for a syngas feed containing a high concentration of hydrogen sulphide, as the Fe or Cu based catalysts would exhibit significant reduction in the reaction rates as well as lose the catalytic activity greatly when exposed to H_2S [27].

As for the sour shift, a Co-Mo based catalyst ($CoO/MoO_3/MgO/Al_2O_3$/promoter = 2:8:24:50:balance wt%), referred to SSC, was chosen, as this catalyst's activity could be promoted by the sulphur compounds contained in a syngas feed. Hla et al. [34] carried out experiments to measure the shift reaction rates of gases containing 1000 H_2S ppmv on SSC in the range of 350 – 450 °C and at 101.32 kPa. They proposed that the reaction rate could be estimated by a power-law model as follows [34]:

$$r_{SSC,1000ppmv\,H_2S} = 0.008e^{\frac{-60300}{RT}} P_{CO}^{0.75} P_{H_2O}^{0.31} P_{CO_2}^{-0.07} P_{H_2}^{-0.09} \left(1 - \frac{1}{K_e}\frac{P_{CO_2}P_{H_2}}{P_{CO}P_{H_2O}}\right) \quad (5)$$

Hla et al. [34] also investigated the effect of H_2S on the shift reaction rates with the H_2S concentration in the feed gas varied from 330 to 2670 ppmv. When plotted in log-log graph, the experimental data exhibited linearity. Accordingly, the effect of H_2S on the reaction rate is expressed by

$$r_{SSC} = r_{SSC,1000ppmv\,H_2S}\left[\frac{H_2S\ ppmv}{1000}\right]^n \quad (6)$$

where n is the slope of the trend line in the logarithmic coordinate, estimated 0.52 in their experimental study [34]. Similarly to the study on the sweet shift catalysts, the pressure correction factor, Eq. 4, was applied to the reaction rate models, in order to estimate the reaction rates at the very high pressure from those estimated at ambient pressure for sizing the high-pressure reactor. It was assumed that the SSC catalysts be applicable to both HTSR and LTSR in sour shift case.

For simplicity, it was assumed that all three catalysts had identical particle density (2400 kg/m^3) and bulk density (1200 kg/m^3). Also the following assumptions were made: no pressure drop, adiabatic reactors, plug flow, no radial distributions of temperature and concentration, negligible mass transfer resistances at the film and in the pore and no axial dispersion.

3.3. Comparison of the Sweet and Sour Shift Reactors

With the assumptions made above, a reactor size is to be estimated only by a plug flow reactor model including the shift reaction rate model. First, the chosen rate models were tested to see if they could replicate the experimental results reported in the references. Hla et al. [27] measured the CO conversion rate at 450 °C and 1 atm when a dry-feed coal-derived syngas was fed to a lab-scale reactor packed with HTC1 in the conditions of the actual gas space velocity of 1.9 m^3 gcat^{-1} h^{-1} and the steam-to-carbon ratio of around 3. The experimental CO conversion was reported around 7.8%, while its equivalent simulation of this study resulted in 5.6% CO conversion assuming isothermal operation.

Hla et al. [34] tested the SSC1 catalyst with a dry-feed coal-derived syngas containing 1000 ppmv H_2S at 450 °C and 1 atm with the steam-to-carbon ratio adjusted to 3. The experimental CO conversion rate was around 1.5 mol gcat^{-1} s^{-1}, while its value estimated by UniSim PFR was 1.1 mol gcat^{-1} s^{-1}.

As for the Cu-based catalyst, Mendes et al. [28] reported the CO conversion rates when a typical reformate gas was fed to a lab-scale reactor at 1.2 bar with both the reaction temperature and the contact time varied. Again, the experimental results were compared with the simulation results by solving the reaction rate model applicable to a broader temperature range, 180 – 300 °C, with UniSim PFR. The PFR simulation results were

slightly lower than the experimental CO conversion rates, as the differences between the two were within 6% points in most data. For example, the UniSim PFR estimated the CO conversion rate of 44%, while the experimental value was 48%, at the contact time of 12.9 gcat h mol^{-1} and 200 °C.

In those papers proposing the reaction rate equations, each parameter was reported as an average value that is allowed to vary in a range. By adjusting the parameters within their associated ranges, it might be possible to make the simulation results closer to the experimental results. In this study, however, such laborious works were not attempted on the grounds that when the reaction rate models were implemented with the average parameter values, they could reproduce the experimental results reasonably well. Again this part of study was aimed to estimate roughly the amount of shift catalysts required to achieve the desired CO conversion rate in the sweet and sour shift cases.

In this study, the volume of a shift reactor was determined so that the CO conversion rate could reach 99% of the equilibrium conversion for all four reactors. Table 6 summarises the simulation results of all four shift reactors and Figure 7 shows the CO mole fraction profiles along the reactor volume in the high and low temperature shift reactors of both cases. As for the high temperature shift reactors, the volumes of the two reactors were relatively close to each other. The reactor volumes were estimated 84.7 m^3 and 56.8 m^3 for the sweet shift reactor and the sour shift reactor, respectively. As explained above, it is essential to incorporate the H_2S correction factor, Eq. 6, into the reaction rate equation in sour shift case, as the reaction rate would be promoted greatly by the presence of H_2S in the feed. Otherwise, the CO conversion rate plunged to 34% from 77% in the same reactor.

However, the reactor lengths required for low temperature shift reaction were very different between the two shift cases. It was estimated that the reactor packed with the Cu-based catalysts for sweet shift would require only 60.6 m^3, while the sour shift reactor with the CoMo-based catalysts had to be 615.8 m^3 in volume. This is due to the reaction rate model found for the sour shift catalyst predicting very low reaction rates in the temperature range of the LTSR as shown in Table 6. This puzzling result indicates that the chosen CoMo catalysts would be effective only in the temperature ranges well above the LTSR temperature [35] and other sulphur-resistant catalysts must be taken for the LTSR. Such catalysts may be commercially available, but to

the best of our knowledge their reaction rate models have not been reported in open literatures yet.

Table 6. Size of the shift reactors estimated by the reaction rate models at the condition of 99% approach to the equilibrium CO conversion.

	Sweet HTSR	**Sweet LTSR**	**Sour HTSR**	**Sour LTSR**
Catalyst	**HTC1 (Fe-based catalyst)**	**LTS (Cu-based catalyst)**	**SSC (CoMo-based catalyst)**	**SSC (CoMo-based catalyst)**
Volume, m^3	84.7	60.6	56.8	615.8
CO conversion rate	77.9%	78.4%	77.1%	78.5%
Average reaction rate, $mol/cm^3/s$	$2.78 \cdot 10^{-5}$	$8.63 \cdot 10^{-6}$	$4.11 \cdot 10^{-5}$	$8.83 \cdot 10^{-7}$

4. Conclusions

In this study, the two process configurations of an IGCC integrated with either sour or sweet shift catalytic reactors were designed, to see which alterations to be made to syngas cooling, shift reactors, acid gas removal unit and steam cycle. Based on the detailed process flowsheets, the energy penalty incurred by carbon capture integration was estimated more accurately than ever. As expected, the sweet shift case would require a far greater amount of additional shift steam than the sour shift case. Contrary to the stereotype of sweet shift resulting in a greater energy penalty than sour shift, however, the energy penalties incurred by carbon capture integration were estimated almost equal in both shift cases. This was mainly due to the sweet shift case not requiring syngas quenching. Note that if the sweet shift case would be configured in the same way as the sour shift case up to the syngas scrubber stage, including water quenching and operating the syngas scrubber at the higher temperature, the sweet shift case would incur 3.7% points greater energy penalty than the sour shift case. However, either syngas quenching or high temperature operation of the syngas scrubber are not required for sweet shift case.

The CO_2 absorber of the DS Selexol process runs with two solvents: lean solvent and semi-lean solvent. The two solvent flowrates are complementary to each other, i.e. increasing the lean solvent flowrate allows to reduce the semi-lean flowrate or vice versa. Accordingly, the DS Selexol process could be designed in two different modes: high lean or low lean modes. In the sweet shift case, however, the low lean mode has to be

chosen, as the amount of CO_2 transferred to the syngas from the solvent taking place at the H_2S absorber must be minimised. Otherwise, the syngas leaving the H_2S absorber would contain more CO_2, requiring more shift stream to be added for the ensuing shift reactors. With respect to the process configuration, the sweet shift case does not need to have a H_2S concentrator separately, as the H_2S absorber also functions as enriching H_2S in the H_2S-laden solvent by stripping CO_2 off the solvent.

In sizing the shift reactors with the reaction rate models found in the literatures, it was found that the sizes of the high-temperature shift reactors are comparable to each other. However, the low temperature sour shift reactor had to be sized much larger than the equivalent sweet shift reactor, due to the sour shift catalysts exhibiting one order of magnitude lower reaction rates than the sweet catalysts in the operating conditions of the catalytic reactor. However, all the reactor sizing of this study may need to be updated afterwards, once the latest shift catalysts are experimented and their reaction rate models are found and reported. In this study, the CoMo catalyst performing excellently at high temperatures were also taken for the low temperature shift reactor of the sour shift case, as to the best of our knowledge any other catalysts suitable for this reactor had not been put forward with the reaction rate model as yet.

Acknowledgements

Financial support from EPSRC grant (EP/N024672/1) is gratefully acknowledged.

References

[1] Demirbas A. Potential applications of renewable energy sources, biomass combustion problems in boiler power systems and combustion related environmental issues[Progress in Energy and Combustion Science. 2005;31(2):171-92.

[2] Shafiee S, Topal E. When will fossil fuel reserves be diminished? Energy Policy. 2009;37(1):181-9.

[3] Müller S, Brown A, Ölz S. Renewable energy: Policy considerations for deploying renewables. Paris, France: International Energy Agency. 2011.

[4] Olah GA. Beyond oil and gas: the methanol economy. Angew Chem Int Ed Engl. 2005;44(18):2636-9.

[5] DOE/NETL. Cost and performance baseline for fossil energy plants. Volume 1: Bituminous coal and natural gas to electricity final report. National Energy Technology Laboratory. 2007.

[6] DOE/NETL. Cost and performance baseline for fossil energy plants volume 1: bituminous coal and natural gas to electricity Revision 2. 2010.

[7] Black J. Cost and performance baseline for fossil energy plants volume 1: bituminous coal and natural gas to electricity. National Energy Technology Laboratory: Washington, DC, USA. 2010.

[8] Guardian T. No new coal without catbon capture, UK government rules. 2009.

[9] Blomen E, Hendriks C, Neele F. Capture technologies: Improvements and promising developments. Enrgy Proced. 2009;1(1):1505 - 12.

[10] NETL D. Water gas shift & hydrogen production.

[11] Descamps C, Bouallou C, Kanniche M. Efficiency of an Integrated Gasification Combined Cycle (IGCC) power plant including CO2 removal. Energy. 2008;33(6):874-81.

[12] Hallmark B, Parra-Garrido J, Murdoch A, Salmon I, Hodrien C. Benchmarking the Timmins Process - a novel approach for low energy pre-combustion carbon capture in IGCC flowsheets. Canadian Journal of Chemical Engineering. 2017;95(6):1023-33.

[13] Sheikh HM, Ullah A, Hong K, Zaman M. Thermo-economic analysis of integrated gasification combined cycle (IGCC) power plant with carbon capture. Chemical Engineering and Processing. 2018;128:53-62.

[14] Trapp C, Thomaser T, van Dijk HAJ, Colonna P. Design optimization of a pre-combustion CO2 capture plant embedding experimental knowledge. Fuel. 2015;157:126-39.

[15] Kanniche M, Bouallou C. CO2 capture study in advanced integrated gasification combined cycle. Applied Thermal Engineering. 2007;27(16):2693-702.

[16] Huang Y, Rezvani S, McIlveen-Wright D, Minchener A, Hewitt N. Techno-economic study of CO2 capture and storage in coal fired oxygen fed entrained flow IGCC power plants. Fuel Processing

Technology. 2008;89(9):916-25.
[17] Cormos CC, Cormos AM, Agachi S. Power generation from coal and biomass based on integrated gasification combined cycle concept with pre- and post-combustion carbon capture methods. Asia-Pacific Journal of Chemical Engineering. 2009;4(6):870-7.
[18] Cormos C-C, Agachi PS. Integrated assessment of carbon capture and storage technologies in coal-based power generation using CAPE tools. Computer Aided Chemical Engineering: Elsevier; 2012. p. 56-60.
[19] Padurean A, Cormos CC, Agachi PS. Pre-combustion carbon dioxide capture by gas-liquid absorption for Integrated Gasification Combined Cycle power plants. International Journal of Greenhouse Gas Control. 2012;7:1-11.
[20] Prins M, Van den Berg R, Van Holthoon E, Van Dorst E, Geuzebroek F. Technological Developments in IGCC for Carbon Capture. Chemical Engineering & Technology. 2012;35(3):413-9.
[21] Beavis R, Forsyth J, Roberts E, Song B, Combes G, Abbott J, et al. A Step-change Sour Shift process for improving the efficiency of IGCC with CCS. Enrgy Proced. 2013;37:2256-64.
[22] Bucklin RW, Shendel, R.L. Comparison of fluor solvent and Selexol processes. Energy Progress. 1984;4:137-42.
[23] Ahn H. Process Simulation of a Dual-stage Selexol Process for Pre-combustion Carbon Capture at an Integrated Gasification Combined Cycle Power Plant. Process Systems and Materials for CO2 Capture: Modelling, Design, Control and Integration. 2017:609-28.
[24] Ahn H, Kapetaki Z, Brandani P, Brandani S. Process simulation of a dual-stage Selexol unit for pre-combustion carbon capture at an IGCC power plant. Enrgy Proced. 2014;63:1751-5.
[25] Kapetaki Z, Brandani P, Brandani S, Ahn H. Process simulation of a dual-stage Selexol process for 95% carbon capture efficiency at an integrated gasification combined cycle power plant. International Journal of Greenhouse Gas Control. 2015;39:17-26.
[26] Kapetaki Z, Ahn H, Brandani S. Detailed process simulation of pre-combustion IGCC plants using coal-slurry and dry coal gasifiers. Enrgy Proced. 2013;37:2196-203.
[27] Hla SS, Park D, Duffy GJ, Edwards JH, Roberts DG, Ilyushechkin A, et al. Kinetics of high-temperature water-gas shift reaction over two iron-based commercial catalysts using simulated coal-derived syngases. Chemical Engineering Journal. 2009;146(1):148-54.
[28] Mendes D, Chibante V, Mendes A, Madeira LM. Determination of the Low-Temperature Water-Gas Shift Reaction Kinetics Using a Cu-Based Catalyst. Industrial & Engineering Chemistry Research. 2010;49(22):11269-79.
[29] Twigg MV, Spencer MS. Deactivation of supported copper metal catalysts for hydrogenation reactions. Applied Catalysis a-General. 2001;212(1-2):161-74.
[30] Singh CPP, Saraf DN. Simulation of High-Temperature Water-Gas Shift Reactors. Industrial & Engineering Chemistry Process Design and Development. 1977;16(3):313-9.
[31] Singh CPP, Saraf DN. Simulation of Low-Temperature Water-Gas Shift Reactor. Industrial & Engineering Chemistry Process Design and Development. 1980;19(3):393-6.
[32] Adams II TA, Barton PI. A dynamic two-dimensional heterogeneous model for water gas shift

reactors. International Journal of Hydrogen Energy. 2009;34(21):8877-91.
[33] Mobed P, Maddala J, Rengaswamy R, Bhattacharyya D, Turton R. Data Reconciliation and Dynamic Modeling of a Sour Water Gas Shift Reactor. Industrial & Engineering Chemistry Research. 2014;53(51):19855-69.
[34] Hla SS, Duffy GJ, Morpeth LD, Cousins A, Roberts DG, Edwards JH. Investigation into the performance of a Co-Mo based sour shift catalyst using simulated coal-derived syngases. International Journal of Hydrogen Energy. 2011;36(11):6638-45.
[35] Plaza A, Fail S, Cortes JA, Fottinger K, Diaz N, Rauch R, et al. Apparent kinetics of the catalyzed water-gas shift reaction in synthetic wood gas. Chemical Engineering Journal. 2016;301:222-8.

Figure

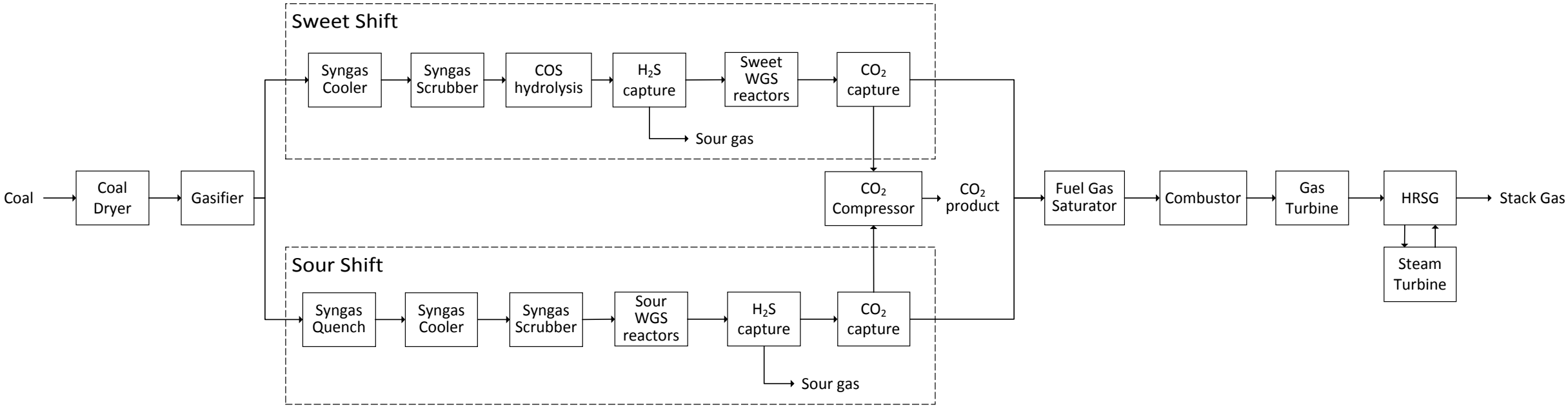

Figure 1. Block flow diagram of pre-combustion capture IGCCs configured based on either sweet or sour shift.

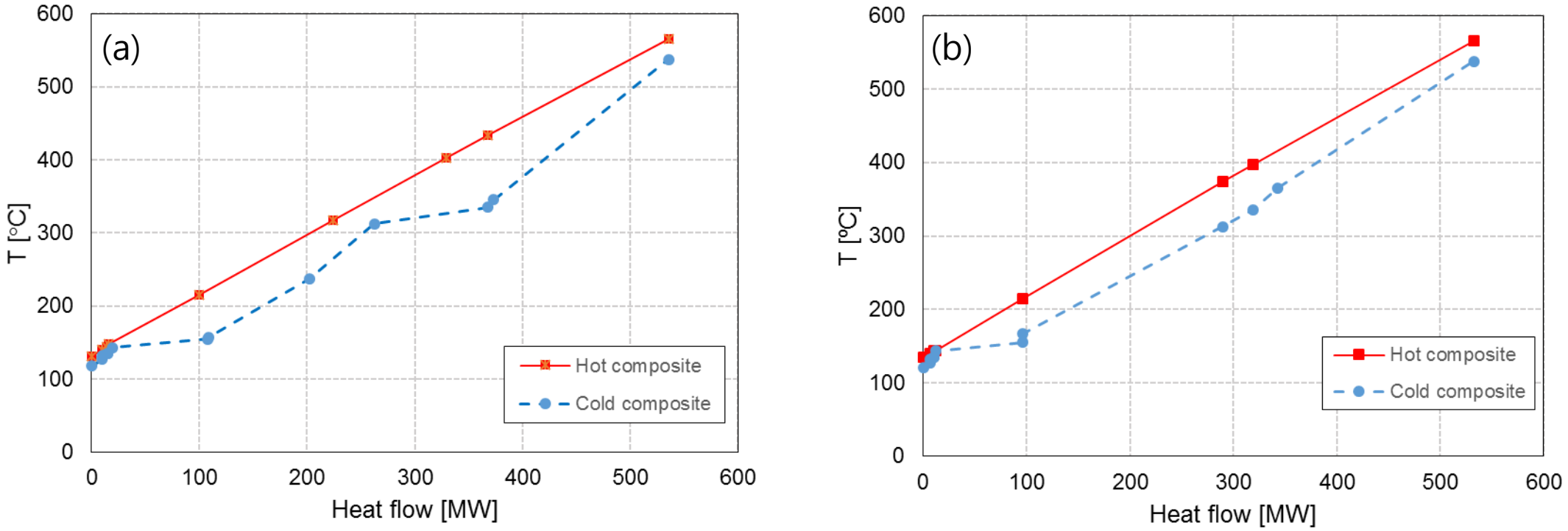

Figure 2. Hot and cold composite curves of HSRG of (a) sour shift case and (b) sweet shift case.

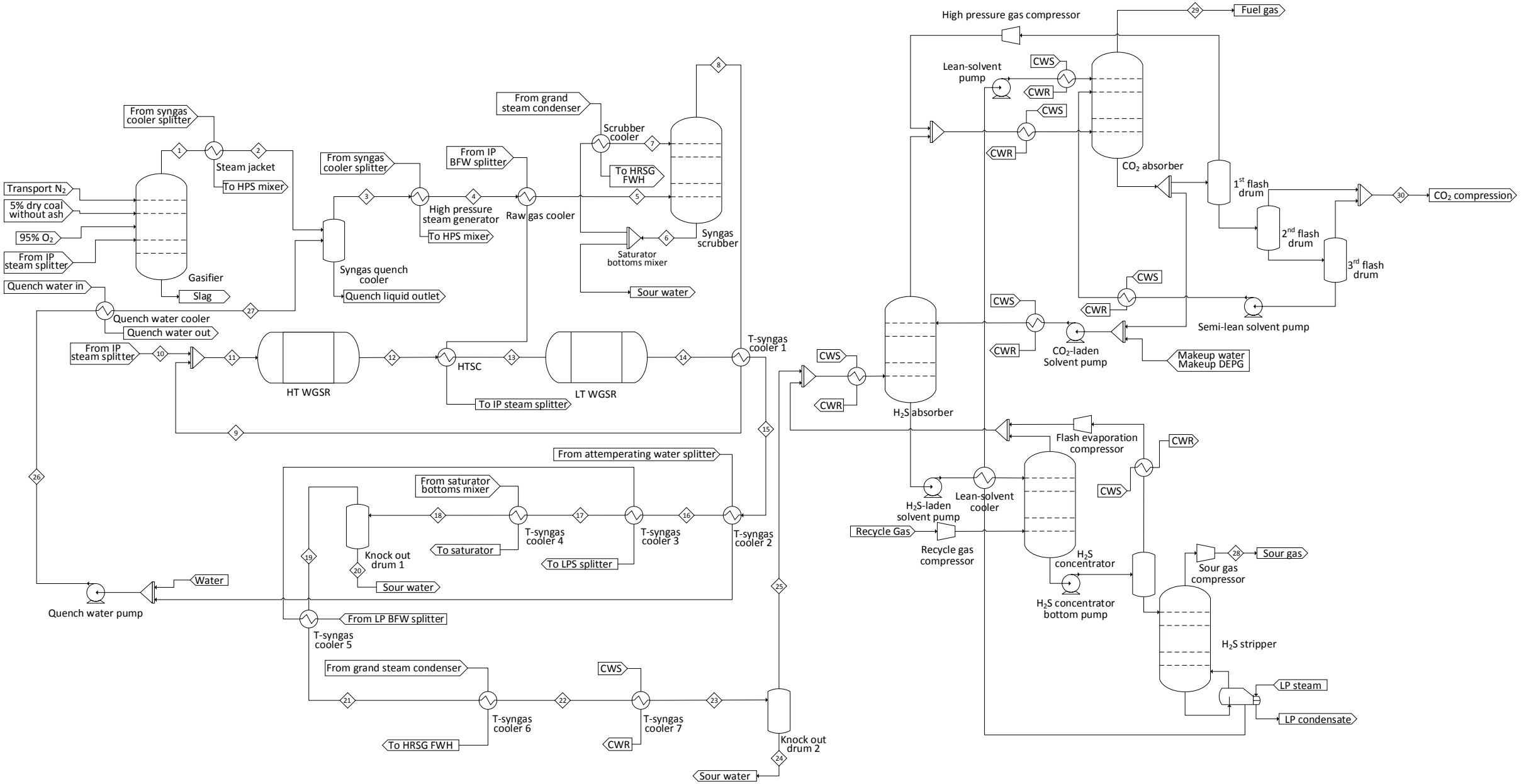

Figure 3. Gas stream flow of the gasification and syngas processing sections: sour shift case.

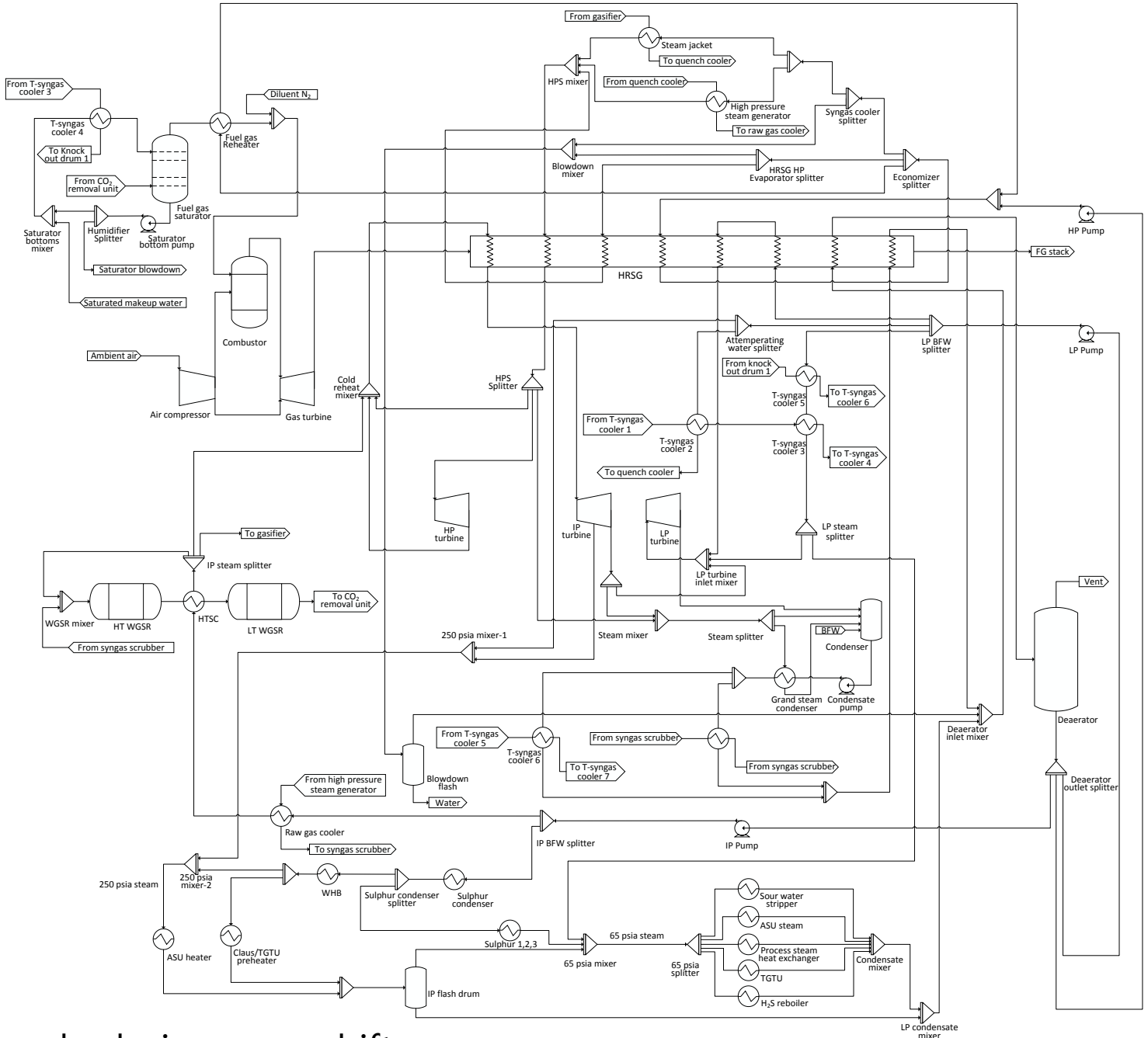

Figure 4. Steam cycle design: sour shift case.

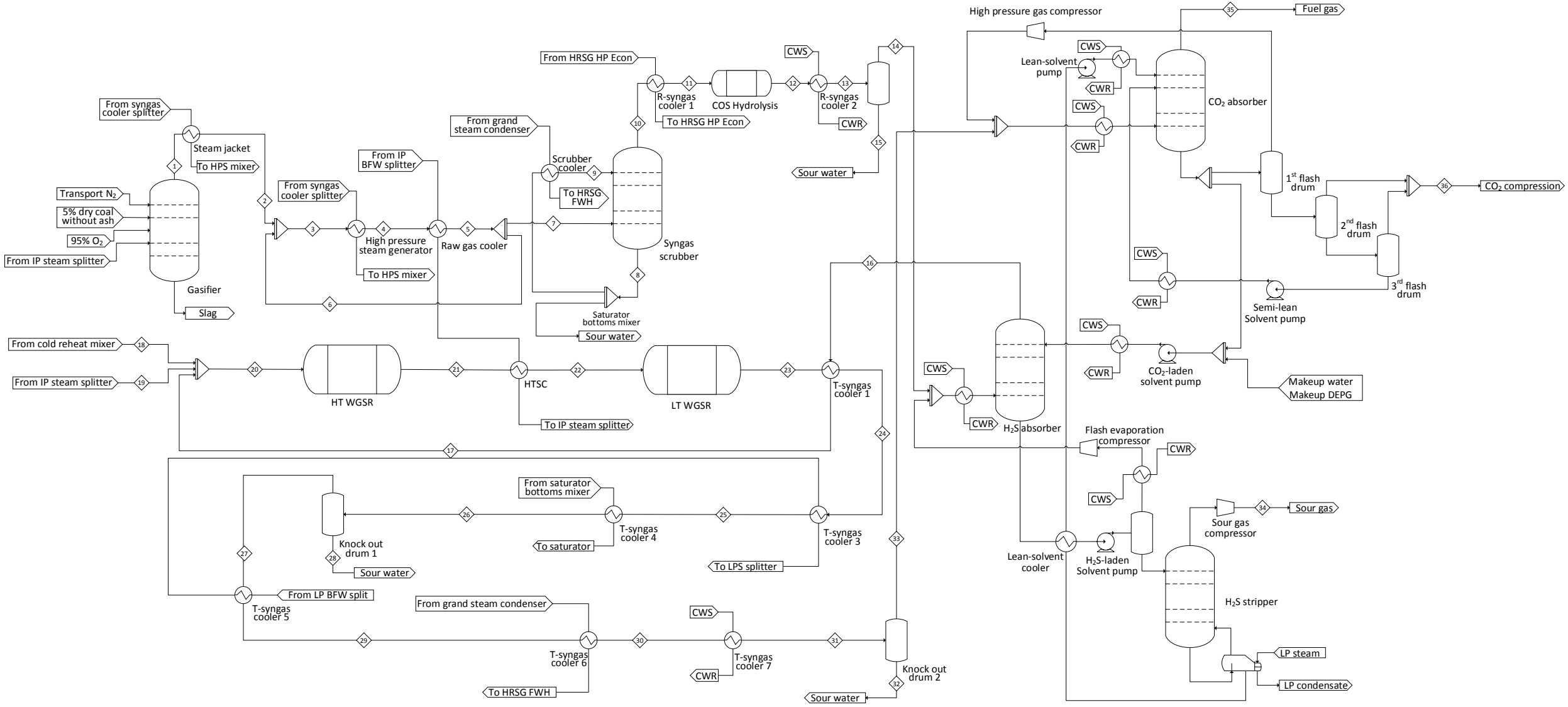

Figure 5. Gas stream flow of the gasification and syngas processing sections: sweet shift case.

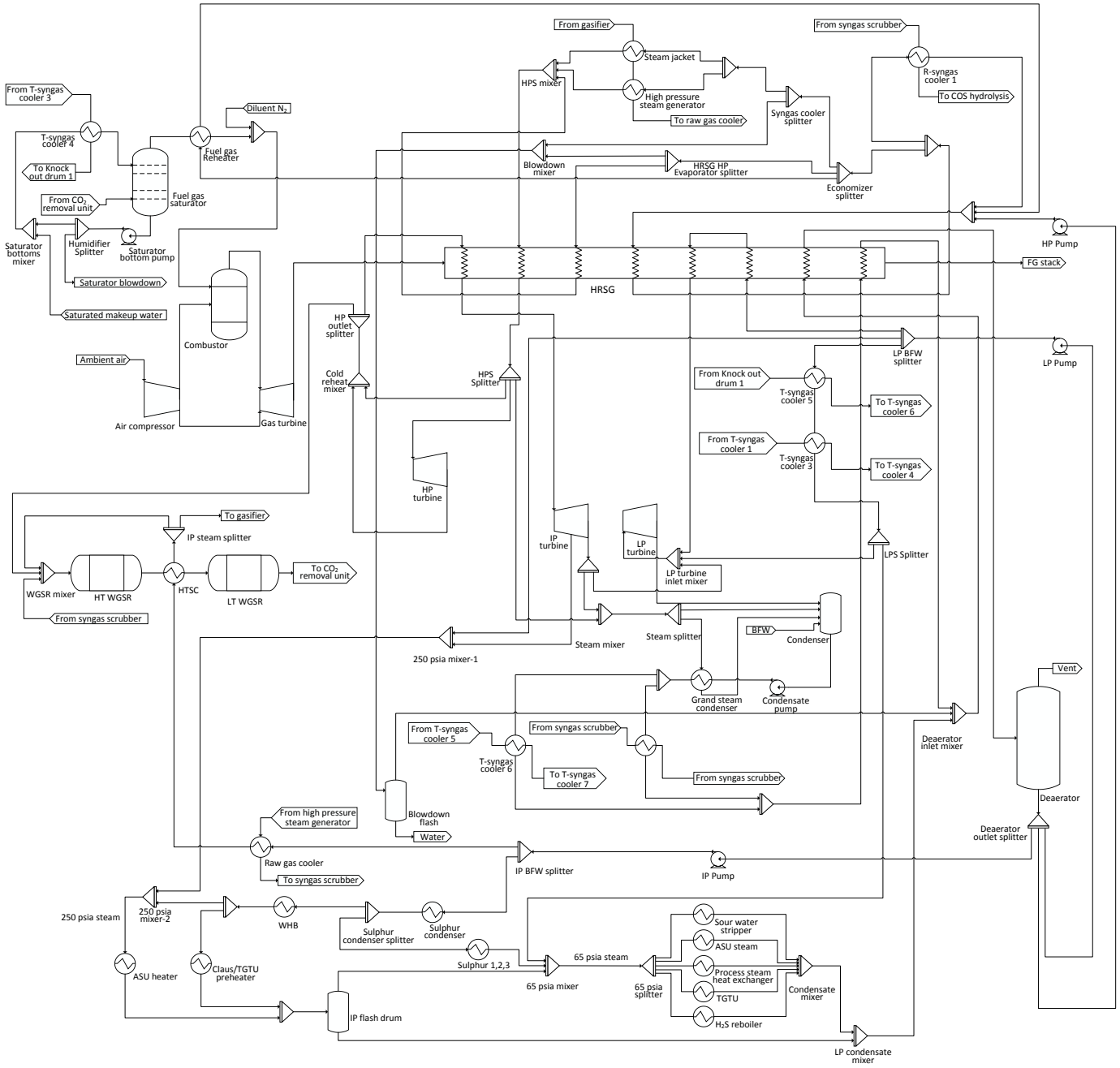

Figure 6. Steam cycle design: sweet shift case.

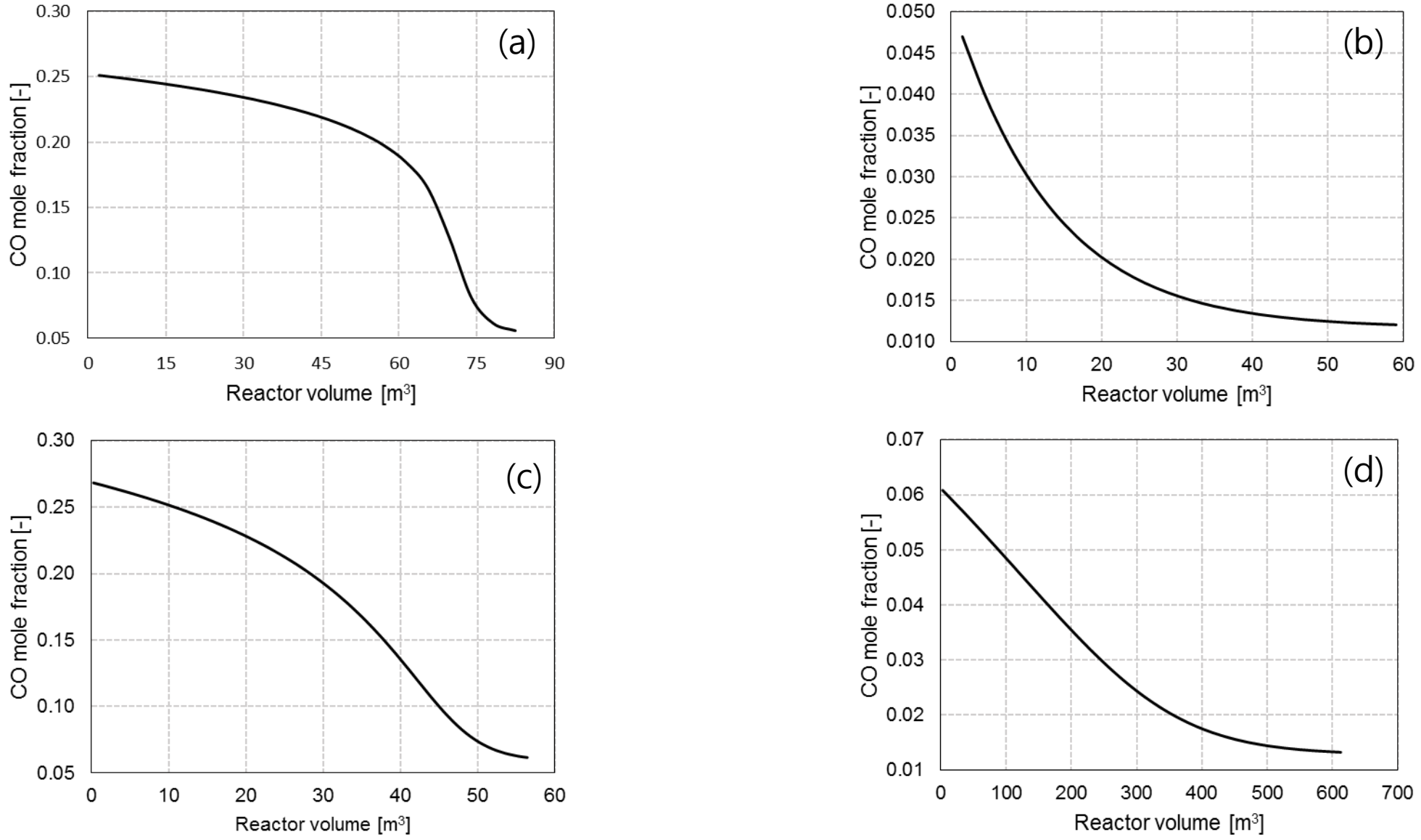

Figure 7. Profiles of CO component mole fractions along the reactor volume: (a) high temperature sweet shift on Fe-based catalysts, (b) low temperature sweet shift on Cu-based catalysts, (c) high temperature sour shift on CoMo-based catalysts, (d) low temperature sour shift on CoMo-based catalysts.

Supplementary Material

Click here to download Supplementary Material: Supplementary materials-new.docx

Supplementary materials - The Implications of Choice between Sour and Sweet Shift on Process Design and Operation of an IGCC Power Plant Integrated with a Dual-Stage Selexol Unit by Y. Zhang and H. Ahn.

Table S1. Temperature, pressure, molar flowrate and mole fraction of each stream in sweet case.

Stream number	**1**	**2**	**3**	**4**	**5**	**6**	**7**	**8**	**9**	**10**	**11**	**12**	**13**	**14**	**15**	**16**	**17**	**18**
T (°C)	1601	1424	898	316	230	246	230	139	42	117	177	177	35	35	35	30	223	365
P (kPa)	4238	4238	4238	4031	3893	4240	3893	3893	3893	3756	3576	3756	3756	3756	3756	3750	3750	3800
Flowrate (kmol/h)	1.91E+04	1.91E+04	3.56E+04	3.56E+04	3.56E+04	1.66E+04	1.91E+04	6.82E+03	7.20E+03	1.94E+04	1.94E+04	1.94E+04	1.94E+04	1.84E+04	1.05E+03	1.96E+04	1.96E+04	1.44E+04
Mole fraction																		
Argon	0.0097	0.0097	0.0097	0.0097	0.0097	0.0097	0.0097	0	0	0.0095	0.0095	0.0095	0.0095	0.0101	0	0.0095	0.0095	0
Methane	0.0004	0.0004	0.0004	0.0004	0.0004	0.0004	0.0004	0	0	0.0004	0.0004	0.0004	0.0004	0.0004	0	0.0004	0.0004	0
CO	0.5720	0.5720	0.5720	0.5720	0.5720	0.5720	0.5720	0.0001	0.0001	0.5608	0.5608	0.5608	0.5608	0.5929	0.0003	0.5555	0.5555	0
CO_2	0.0211	0.0211	0.0211	0.0211	0.0211	0.0211	0.0211	0.0001	0.0001	0.0207	0.0207	0.0214	0.0214	0.0226	0.0003	0.0913	0.0913	0
COS	0.0007	0.0007	0.0007	0.0007	0.0007	0.0007	0.0007	0	0	0.0007	0.0007	0	0	0	0	0	0	0
H_2	0.2899	0.2899	0.2899	0.2899	0.2899	0.2899	0.2899	0	0	0.2842	0.2842	0.2842	0.2842	0.3005	0.0006	0.2871	0.2871	0
H_2O	0.0364	0.0364	0.0364	0.0364	0.0364	0.0364	0.0364	0.9960	0.9962	0.0553	0.0553	0.0546	0.0546	0.0023	0.9687	0.0002	0.0002	1
H_2S	0.0081	0.0081	0.0081	0.0081	0.0081	0.0081	0.0081	0.0001	0.0001	0.0080	0.0080	0.0086	0.0086	0.0091	0.0004	0	0	0
N_2	0.0574	0.0574	0.0574	0.0574	0.0574	0.0574	0.0574	0	0	0.0563	0.0563	0.0563	0.0563	0.0595	0.0000	0.0561	0.0561	0
Ammonia	0.0033	0.0033	0.0033	0.0033	0.0033	0.0033	0.0033	0.0036	0.0034	0.0032	0.0032	0.0032	0.0032	0.0017	0.0297	0	0	0
O_2	0	0	0	0	0	0	0	0	0	0	0	0	0	0	0	0	0	0
Carbon	0	0	0	0	0	0	0	0	0	0	0	0	-	-	-	0	0	0
Sulphur (Rhombic)	0	0	0	0	0	0	0	0	0	0	0	0	-	-	-	0	0	0
Cl_2	0	0	0	0	0	0	0	0	0	0	0	0	-	-	-	0	0	0
HCl	0.0009	0.0009	0.0009	0.0009	0.0009	0.0009	0.0009	0	0	0.0009	0.0009	0.0009	0	0	0	0	0	0
SO_2	-	-	-	-	-	-	-	-	-	-	-	-	0.0009	0.0010	0	-	-	-

Table S2. Temperature, pressure, molar flowrate and mole fraction of each stream in sweet case (continued).

Stream number	**19**	**20**	**21**	**22**	**23**	**24**	**25**	**26**	**27**	**28**	**29**	**30**	**31**	**32**	**33**	**34**	**35**	**36**
T (°C)	399	307	510	271	314	239	162	158	157	157	156	93	35	35	35	88	26	30
P (kPa)	5688	3750	3750	3652	3652	3569	3500	3500	3496	3496	3396	3396	3396	3323	3323	166	3248	345
Flowrate (kmol/h)	9.03E+03	4.31E+04	4.31E+04	4.31E+04	4.31E+04	4.31E+04	4.31E+04	4.31E+04	3.68E+04	6.28E+03	3.68E+04	3.68E+04	3.68E+04	6.72E+03	3.01E+04	3.39E+02	1.79E+04	1.05E+04
Mole fraction																		
Argon	0	0.0043	0.0043	0.0043	0.0043	0.0043	0.0043	0.0043	0.0050	0	0.0050	0.0050	0.0050	0	0.0062	0	0.0103	0.0000
Methane	0	0.0002	0.0002	0.0002	0.0002	0.0002	0.0002	0.0002	0.0002	0	0.0002	0.0002	0.0002	0	0.0003	0.0001	0.0004	0.0001
CO	0	0.2529	0.0523	0.0523	0.0110	0.0110	0.0110	0.0110	0.0129	0	0.0129	0.0129	0.0129	0	0.0158	0.0362	0.0254	0.0014
CO_2	0	0.0415	0.2421	0.2421	0.2834	0.2832	0.2832	0.2832	0.3313	0.0015	0.3313	0.3313	0.3313	0.0006	0.4052	0.3730	0.0279	0.9683
COS	0	0	0	0	0	0	0	0	0	0	0	0	0	0	0	0	0	0
H_2	0	0.1307	0.3313	0.3313	0.3725	0.3726	0.3726	0.3726	0.4362	0.0001	0.4362	0.4362	0.4362	0.0000	0.5337	0.0100	0.8756	0.0212
H_2O	1	0.5448	0.3443	0.3443	0.3030	0.3031	0.3031	0.3031	0.1844	0.9985	0.1844	0.1844	0.1844	0.9994	0.0022	0.0847	0.0004	0.0075
H_2S	0	0	0	0	0	0	0	0	0	0	0	0	0	0	0	0.4946	0.0000	0.0000
N2	0	0.0255	0.0255	0.0255	0.0255	0.0255	0.0255	0.0255	0.0299	0.0000	0.0299	0.0299	0.0299	0.0000	0.0366	0.0014	0.0601	0.0014
Ammonia	0	0	0	0	0	0	0	0	0	0	0	0	0	0	0	0	0	0
O_2	0	0	0	0	0	0	0	0	0	0	0	0	0	0	0	0	0	0
Carbon	0	0	0	0	0	0	0	0	0	0	0	0	0	0	0	-	-	-
Sulphur (Rhombic)	0	0	0	0	0	0	0	0	0	0	0	0	0	0	0	-	-	-
Cl_2	0	0	0	0	0	0	0	0	0	0	0	0	0	0	0	-	-	-
HCl	0	0	0	0	0	0	0	0	0	0	0	0	0	0	0	0	0	0
SO_2	-	-	-	-	-	-	-	-	-	-	-	-	-	-	-	0	0	0

Table S3. Temperature, pressure, molar flowrate and mole fraction of each stream in sour case.

Stream number	**1**	**2**	**3**	**4**	**5**	**6**	**7**	**8**	**9**	**10**	**11**	**12**	**13**	**14**	**15**
T (°C)	1601	1424	408	343	266	209	43	204	298	399	310	527	270	317	239
P (kPa)	4238	4169	4031	3962	3893	3893	3893	3756	3756	5688	3756	3756	3652	3652	3569
Flowrate (kmol/h)	1.91E+04	1.91E+04	3.55E+04	3.55E+04	3.55E+04	7.20E+03	6.89E+03	3.52E+04	3.52E+04	5.30E+03	4.05E+04	4.05E+04	4.05E+04	4.05E+04	4.05E+04
Mole fraction															
Argon	0.0097	0.0097	0.0052	0.0052	0.0052	0	0	0.0053	0.0053	0	0.0046	0.0046	0.0046	0.0046	0.0046
Methane	0.0004	0.0004	0.0002	0.0002	0.0002	0	0	0.0002	0.0002	0	0.0002	0.0002	0.0002	0.0002	0.0002
CO	0.5720	0.5720	0.3070	0.3070	0.3070	0.0002	0.0002	0.3096	0.3096	0	0.2691	0.0573	0.0573	0.0120	0.0120
CO_2	0.0211	0.0211	0.0113	0.0113	0.0113	0.0001	0.0001	0.0114	0.0114	0	0.0099	0.2218	0.2218	0.2670	0.2670
COS	0.0007	0.0007	0.0004	0.0004	0.0004	0	0	0.0004	0.0004	0	0.0003	0.0003	0.0003	0.0003	0.0003
H_2	0.2899	0.2899	0.1556	0.1556	0.1556	0.0001	0.0001	0.1569	0.1569	0	0.1364	0.3483	0.3483	0.3935	0.3935
H_2O	0.0364	0.0364	0.4828	0.4828	0.4828	0.9989	0.9989	0.4784	0.4784	1	0.5466	0.3348	0.3348	0.2895	0.2895
H_2S	0.0081	0.0081	0.0044	0.0044	0.0044	0.0001	0.0001	0.0044	0.0044	0	0.0038	0.0038	0.0038	0.0038	0.0038
N_2	0.0574	0.0574	0.0308	0.0308	0.0308	0	0	0.0311	0.0311	0	0.0270	0.0270	0.0270	0.0270	0.0270
Ammonia	0.0033	0.0033	0.0018	0.0018	0.0018	0.0006	0.0006	0.0018	0.0018	0	0.0016	0.0016	0.0016	0.0016	0.0016
O_2	0	0	0	0	0	0	0	0	0	0	0	0	0	0	0
Carbon	0	0	0	0	0	0	0	0	0	0	0	0	0	0	0
Sulphur (Rhombic)	0	0	0	0	0	0	0	0	0	0	0	0	0	0	0
Cl_2	0	0	0	0	0	0	0	0	0	0	0	0	0	0	0
HCl	0.0009	0.0009	0.0005	0.0005	0.0005	0	0	0.0005	0.0005	0	0.0004	0.0004	0.0004	0.0004	0.0004
SO_2	-	-	-	-	-	-	-	-	-	-	-	-	-	-	-

Table S4 Temperature, pressure, molar flowrate and mole fraction of each stream in sour case (continued).

Stream number	**16**	**17**	**18**	**19**	**20**	**21**	**22**	**23**	**24**	**25**	**26**	**27**	**28**	**29**	**30**
T (°C)	191.2	154	148	148	148	147	93	35	35	35	132	237.8	87	26	28
P (kPa)	3569	3500	3500	3496	3496	3396	3396	3396	3323	3323	8274	8274	166	3238	345
Flowrate (kmol/h)	4.05E+04	4.05E+04	4.05E+04	3.35E+04	6.98E+03	3.35E+04	3.35E+04	3.35E+04	4.74E+03	2.88E+04	1.65E+04	1.65E+04	4.02E+02	2.14E4	1.04E4
Mole fraction															
Argon	0.0046	0.0046	0.0046	0.0055	0	0.0055	0.0055	0.0055	0	0.0064	0	0	0	0.0103	0
Methane	0.0002	0.0002	0.0002	0.0002	0	0.0002	0.0002	0.0002	0	0.0003	0	0	0	0.0003	0
CO	0.0120	0.0120	0.0120	0.0145	0	0.0145	0.0145	0.0145	0	0.0169	0	0	0.0003	0.0265	0.0011
CO_2	0.2670	0.2670	0.2670	0.3224	0.0013	0.3224	0.3224	0.3224	0.0006	0.3754	0	0	0.5178	0.0243	0.9739
COS	0.0003	0.0003	0.0003	0.0004	0	0.0004	0.0004	0.0004	0	0.0005	0	0	0	0	0
H_2	0.3935	0.3935	0.3935	0.4755	0	0.4755	0.4755	0.4755	0	0.5539	0	0	0.0139	0.8778	0.0185
H_2O	0.2895	0.2895	0.2895	0.1420	0.9972	0.1420	0.1420	0.1420	0.9910	0.0022	1	1	0.0861	0.0003	0. 0054
H_2S	0.0038	0.0038	0.0038	0.0046	0.0001	0.0046	0.0046	0.0046	0	0.0054	0	0	0.3816	0	0
N_2	0.0270	0.0270	0.0270	0.0326	0	0.0326	0.0326	0.0326	0	0.0380	0	0	0.0003	0.0603	0.0011
Ammonia	0.0016	0.0016	0.0016	0.0016	0.0013	0.0016	0.0016	0.0016	0.0084	0.0005	0	0	0	0	0
O_2	0	0	0	0	0	0	0	0	0	0	0	0	0	0	0
Carbon	0	0	0	0	0	0	0	0	0	0	-	-	-	-	-
Sulphur (Rhombic)	0	0	0	0	0	0	0	0	0	0	-	-	-	-	-
Cl_2	0	0	0	0	0	0	0	0	0	0	-	-	-	-	-
HCl	0.0004	0.0004	0.0004	0.0005	0	0.0005	0.0005	0.0005	0	0.0006	0	0	0	0	0
SO_2	-	-	-	-	-	-	-	-	-	-	0	0	0	0	0

Table S5. Approach points of the main heat exchangers.

Heat exchanger	Approach point (°C)	
	Sour	Sweet
High pressure steam generator	29.8	3.5
Raw gas cooler	92.5	66.3
HTSC	19.8	20.8
T-syngas cooler 1	19.4	91.0
T-syngas cooler 2	12.3	-
T-syngas cooler 3	15.9	24.4
T-syngas cooler 4	52.4	60.9
T-syngas cooler 5	9.7	19.7
T-syngas cooler 6	36.7	22.0
Flue gas reheater	116.7	116.7
Lean-solvent cooler	6.7	50.6
Grand Steam Condenser	1.7	1.7
R-syngas cooler 1	-	136.1
Scrubber cooler	4.2	4.2

Table S6. Summary of adiabatic efficiency of pumps.

Pump	Adiabatic efficiency	
	Sour	Sweet
HP pump	70.2%	70.2%
LP pump	80.0%	80.0%
IP pump	81.0%	81.0%
Condensate pump	63.9%	63.9%
H_2S-laden solvent pump	80.0%	75.0%

H_2S concentrator bottom pump	75.0%	-
CO_2-laden solvent pump	80.0%	80.0%
Lean solvent pump	80.0%	80.0%
Semi-lean solvent pump	80.0%	80.0%
Quench water pump	75.0%	-
CO_2 product pump	85.0%	85.0%
Makeup water pump	75.0%	75.0%
Makeup DEPG pump	75.0%	75.0%

Table S7: Summary of adiabatic efficiency and polytropic efficiency of compressors.

Compressor	**Sour**		**Sweet**	
	Adiabatic efficiency	**Polytropic efficiency**	**Adiabatic efficiency**	**Polytropic efficiency**
Recycle gas compressor	80.0%	80.4%	-	-
Flash evaporation compressor	80.0%	81.7%	80.0%	81.8%
Sour gas compressor	80.0%	81.0%	80.0%	81.0%
High pressure gas compressor	83.4%	85.0%	83.0%	85.0%
Syngas compressor	-	-	75.0%	75.3%
CO_2 compressor-1	83.1%	85.1%	83.1%	85.0%
CO_2 compressor-2	83.7%	85.0%	83.7%	85.0%
CO_2 compressor-3	83.7%	85.0%	83.7%	85.0%
CO_2 compressor-4	83.6%	85.0%	83.6%	85.0%
CO_2 compressor-5	83.6%	85.0%	83.65	85.0%

The Implications of the Choice between Sour and Sweet Shift on Process Design and Operation of an IGCC Power Plant Integrated with a Dual-Stage Selexol Unit

Yixuan Zhang, Hyungwoong Ahn*

School of Engineering, Institute for Materials and Processes,

The University of Edinburgh, Robert Stevenson Road, Edinburgh EH9 3FB, UK

*Corresponding author. Tel.: +44 131 650 5891

E-mail address: H.Ahn@ed.ac.uk

Abstract

In this study, it was sought to design and evaluate two process configurations of an ~~Integrated Gasification Combined Cycle (~~IGCC~~)~~ integrated with a dual-stage Selexol unit in which they differ in that one IGCC is configured with sour shift and the other is based on sweet shift. Incorporating water gas shift reactors consuming vast amount of shift steam into an IGCC involves significant alternations to the associated steam cycle, in addition to simply changing the location of the H_2S removal step around the shift reactors. It turned out that the sweet shift case would require approximately 4.6 times more shift steam than the sour shift case, as the syngas after H_2S removal did not have much steam in it. However, the energy penalties incurred by the carbon capture integration were estimated almost identical regardless of the choice between the sour and sweet shift. This is because the sour shift case would also undergo considerable reduction in power generation at steam cycle due to water quenching. In both shift cases, the high and low temperature shift reactors were sized using the reaction rate models reported in literatures.

Keywords: Carbon capture; Selexol; ~~Process configuration;~~ IGCC; Sour shift reaction; ~~and S~~sweet shift reaction; Reactor design

Nomenclature

K_e	Equilibrium constant (-)
P	Actual system pressure (atm)
P_i	Partial pressure of component i (kPa)
P_t	Pressure correction factor (atm)
r	Reaction rate ($mol/g_{cat} \cdot s$)
R	Ideal gas constant ($J/mol \cdot K$)
T	Temperature (K)

Abbreviation

BFW	Boiler feed water
COS	Carbonyl sulphide
DS	Dual site
DOE	Department of Energy
HP	High pressure
HRSG	Heat recovery steam generator
IP	Intermediate pressure
IGCC	Integrated gasification combined cycle
PC-fired	Pulverized coal fired
SSC	Sour shift catalyst

Formatted: Font: 11 pt

Formatted: Left

1. Introduction

Fossil fuels have long supplied a vast majority of the energy as well as the raw materials our economy needs. With growing concerns with the environmental issues the use of fossil fuels gives rise to, however, it has been sought to replace fossil fuel with renewable resources to enhance sustainability of our society [1]. As various renewable energy technologies have progressed up to commercial stage, it is expected that fossil fuels will lose their position as main energy resources in the future [2]. However, there still remains one aspect that fossil fuels cannot be surpassed by renewables easily. Fossil fuels can produce energy more stably and steadily than renewables, less affected by the weather around the site [3]. Therefore, fossil fuels still play a key role even in the next generation energy mix, supplementing energy production by renewables [2].

As for power generation, coal and natural gas have been the main raw materials among various hydrocarbon fuels [4]. Given the fact that coal reserves are more evenly distributed over the globe than natural gas reserves, use of coal for power generation is expected not to wither in the future even though the plant efficiency of a coal power plant is generally inferior to that of a natural gas combined cycle [5, 6].

However, coals generate the largest CO_2 per unit electricity generated among fossil fuels when combusted for power generation, due to it being characterised by the largest carbon-to-hydrogen ratio [7]. Hence, in the

UK, it has been banned to construct a new coal-based power plant unless its CO_2 emission is to be curtailed significantly by integrating it with carbon capture and storage (CCS) [8]. But CCS is still deemed so expensive that the concept has not been widely materialized into commercialisation yet.

In the chain of CCS, it is known that carbon capture stage accounts for majority of the total energy consumption [9]. Therefore, it is crucial to reduce drastically the energy consumption at carbon capture stage, in order to bring down the overall CCS cost to an affordable level. In this respect, Integrated Gasification Combined Cycle (IGCC) has been considered an attractive alternative to the conventional PC-fired power plant. In IGCC, a pre-combustion capture process can be applied to a synthesis gas (syngas) containing CO_2 at very high pressure. From the thermodynamic point of view, it would be more energy-efficient to separate CO_2 from a high pressure syngas of the IGCC than a low pressure flue gas that a PC-fired power plant emits. In addition, a carbon capture unit can be designed smaller in an IGCC than in a PC-fired power plant, as the high pressure syngas must be smaller in volume than the low pressure flue gas. Accordingly, pre-combustion capture would involve a specific energy consumption less than post-combustion capture. DOE [6] estimated that the cost of electricity (COE) of an IGCC would increase only 35 mills/kWh on average by integrating it with pre-combustion carbon capture, while decarbonising a PC-fired power plant by amine capture would be so expensive that the COE had to increase 49 mills/kWh.

In designing an IGCC integrated with pre-combustion capture, it is essential to include WGSRs (Water-Gas Shift Reactors) to convert CO to CO_2, so that the following CO_2 capture unit can achieve at least 90% capture efficiency. There are largely two different cohorts of shift catalysts available with respect to their resistance to sulphur, that is, sour and sweet shift catalysts. Given the fact the IGCC syngas contains sulphur compounds originating from coals, the syngas has to be cleared of the sulphur species to protect the sweet shift catalysts. As for the choice of sour or sweet shift in decarbonising an IGCC, it was claimed that sweet shift would not be normally taken for coal gasification applications, due to a greater inefficiency arising from having to cool the syngas before the sulphur removal [10]. Most of the past researches on design of an IGCC integrated with pre-combustion capture centred upon sour shift as shown in Table 1. However, there exist a few of works on sweet shift as well, as shown in Table 2 [11-14] .

There have been a few of works carried out to evaluate the sour and sweet shift cases applied to coal gasification for carbon capture. But it appears that the outcomes of the studies are contradictory to each other in contrast to what was expected. Kanniche and Bouallou [15] compared two dry coal IGCC plants integrated with CO_2 capture that were designed based on either sweet or sour shift in terms of net plant efficiency. According to their simulation results, both of the sour and sweet shift cases were estimated to have almost identical net plant efficiencies, with the difference only 0.5-% points. Huang et al. [16] compared the sweet and sour shift options applied to the two IGCC reference plants equipped with either GE or Shell gasification. They reported that the sour shift case would be more efficient than the sweet shift case with its net plant efficiency greater by around 1.5% points.

In this study, it was aimed to estimate the energy penalty of an exemplary IGCC plant integrated with either sour or sweet shift, by designing the entire IGCC process based on the DOE study [5]. By doing so, it was possible to identify which alternations to make in designing the pre-combustion capture IGCCs depending on the choice of sweet or sour shift, and quantify the net plant efficiency more accurately. In addition, the sizes of the shift reactors are to be estimated based on the reaction rate models reported in literatures.

Table 1 Summary of past researches on pre-combustion capture IGCCs based on sour shift.

Ref.	Cormos et. al.[17]				Descamps et.al. [11]				Cormos et.al. [18]			
Plant performance	IGCC only	IGCC + CCS	Energy change	Energy penalty	IGCC only	IGCC + CCS	Energy change	Energy penalty	IGCC only	IGCC + CCS	Energy change	Energy penalty
Thermal input, MW	1053	1177.7	124.7	-	725.8	847.9	122.1	-	1040.9	1166.9	126	-
Power Summary, MW												
Gas turbine power	334	334	0	3.36%	188.3	211.5	23.2	1.00%	334	334	0	3.46%
Steam turbine power	183.6	200.14	16.54	0.44%	152	135.8	-16.2	4.93%	186.92	197.5	10.58	1.03%
Syngas Expander	1.48	0.78	-0.7	0.07%	24.7	29	4.3	0.02%	0.88	0.78	-0.1	0.02%
Total power generation	519.08	534.92	15.84	3.87%	365	376.3	11.3	5.91%	521.8	532.28	10.48	4.51%
Total auxiliaries	75.18	112.99	37.81	2.45%	49.3	82.9	33.6	2.98%	72.83	111.87	39.04	2.59%
Net power	443.9	421.93	-21.97	6.33%	315.7	293.4	-22.3	8.89%	448.97	420.41	-28.56	7.10%
Net power plant efficiency (LHV)	42.16%	35.83%	-	-	43.50%	34.60%	-	-	43.13%	36.03%	-	-

Ref.	Padurean et al. [19]				Huang et al. [16]				Prins et al. [20]			
Plant performance	IGCC only	IGCC + CCS	Energy change	Energy penalty	IGCC only	IGCC + CCS	Energy change	Energy penalty	IGCC only	IGCC + CCS	Energy change	Energy penalty
Thermal input,	1052.9	1177.76	124.86	-	953.3	1066.8	113.5	-	2166.3	2610	443.7	-

Formatted: Font: Bold
Formatted: Font color: Auto
Formatted: Font: Bold
Formatted: Font: Bold

MW												
Power Summary, MW												
Gas turbine power	334	334	0	3.36%	286	286	0	3.19%	720.6	816.6	96	1.98%
Steam turbine power	184.32	195.24	10.92	0.93%	192.4	175.6	-16.8	3.72%	475.2	525.6	50.4	1.80%
Syngas Expander	1.48	0.55	-0.93	0.09%	0	0	0	0.00%	0	0	0	0.00%
Total power generation	519.8	529.79	9.99	4.39%	478.4	461.6	-16.8	6.91%	1195.8	1342.2	146.4	3.77%
Total auxiliaries	75.08	104.82	29.74	1.77%	61.31	94.01	32.7	2.38%	145.1	259.9	114.8	3.26%
Net power	444.72	424.97	-19.75	6.15%	417.09	367.59	-49.5	9.29%	1050.7	1082.3	31.6	7.03%
Net power plant efficiency (LHV)	42.23%	36.09%	-	-	43.75%	34.46%	-	-	48.50%	41.47%	-	-

Table 2 Summary of a pre-combustion capture IGCC based on sweet shift [16].

Plant performance	IGCC only	IGCC + CCS	Energy change	Energy penalty
Thermal input, MW	953.3	1066.8	113.5	-
Power Summary, MW				
Gas turbine power	286	286	0	3.19%
Steam turbine power	192.4	160.9	-31.5	5.10%
Syngas Expander	0	0	0	0.00%
Total power generation	478.4	446.9	-31.5	8.29%
Total auxiliaries	61.31	94.33	33.02	2.41%
Net power	417.09	352.57	-64.52	10.70%
Net power plant efficiency (LHV)	43.75%	33.05%	-	-

2. Process Configuration Studies

2.1. Sour Shift Case

This case was reproduced following the US DOE's work [5] in which the design basis was detailed. In configuring an IGCC, it is essential to select the gas turbine from the beginning. This study is based on two Advanced F class gas turbine to generate 464 MW power in total. The firing temperature of combustion chamber was controlled within the range of 1318-1327°C, with the pressure ratio of 18.5. The net efficiency of such turbines was 57.5% (LHV), giving the net heat rate of 6256 kJ/kWh (LHV). The exhaust gas leaves gas turbine entering the steam cycle via HRSG. The pressure levels for HP/IP/LP sections are 12.5/2.9/0.45 MPa, respectively. In both sour and shift cases, the HRSGs undergo around 533 MW of the heat transfer between the hot and cold streams. The hot and cold composite curves are presented in Figure 2.

~~This case was adopted by various studies listed in Table 1 inclusive of the reference work of this study [5].~~ By taking shift catalysts of which the activity can be maintained high with the presence of sulphur

compound, the shift reactor can process directly the raw syngas containing COS and H_2S without having to pre-treat the syngas but preheating.

In integrating the IGCC with pre-combustion capture, it is essential to make most of the carbon-containing compounds exist in the form of CO_2, as the ensuing carbon capture unit can separate only CO_2 selectively from the gas mixture. To this end the syngas undergoes water-gas shift reaction which often requires a huge amount of steam as much as approximately 2 moles of H_2O per 1 mole of CO [5]. It should be noted that the whole process benefits greatly from the fact that the hot syngas already contains a great deal of steam when leaving the water scrubber operating at high temperature. In this study, the targeted CO conversion rate was set as high as 95.5%, so that the ensuing Selexol process could achieve 90+% carbon capture efficiency easily.

Table 3. Details of the raw syngas flowing into the shift reactor prior to shift steam addition in both sour and sweet shift cases.

	Sour shift case	Sweet shift case
Temperature [°C]	298	223
Pressure [kPa]	3756	3750
Molar flowrate [kmol/s]	9.8	5.4
Molar fraction		
CO	0.3096	0.5560
H_2O	0.4784	0.0002
CO_2	0.0114	0.0908
H_2	0.1569	0.2870
N_2	0.0311	0.0562
H_2S	0.0044	trace
Ar	0.0053	0.0095
CH_4	0.0002	0.0004

Given the syngas composition in Table 3, it is possible to estimate the amount of steam that the syngas must contain in order to achieve the CO conversion efficiency of 95.5%, given the equilibrium constant, ~~K~~K_e, defined by [15]:

$$K_e \sim\sim{K}\sim\sim = e^{\frac{4577.8}{T}-4.33} \quad (1)$$

Assuming the syngas would leave the LTS (Low Temperature Shift) reactor at around 317 °C [5], the

Formatted: Font: 8 pt, Font color Black
Formatted: Font: 8 pt, Bold, Font color: Black
Formatted
Formatted
Formatted Table
Formatted
Formatted
Formatted
Formatted
Formatted
Formatted
Formatted
Formatted
Formatted
Formatted
Formatted
Formatted
Formatted
Formatted
Formatted
Formatted
Formatted
Formatted
Formatted
Formatted
Formatted
Formatted
Formatted
Formatted
Formatted
Formatted
Formatted
Formatted
Formatted
Formatted
Formatted

equilibrium constant was estimated around 31 by Eq. 1. To achieve the K_e ~~K~~ value at 95.5% CO conversion rate, the required amount of steam has to be 6.1 kmol/s, while the flowrate of steam contained in the syngas is only 4.7 kmol/s. Accordingly, around 1.4 kmol/s of steam has to be sourced and supplemented into the syngas. To this end, the ~~intermediate pressure (~~IP~~) boiling feed water (~~BFW~~)~~ is preheated by recovering the heat of the hot raw syngas after ~~high pressure (~~HP~~)~~ steam generation (stream 4 in Figure 2). The hot IP BFW is vaporized to IP steam by recovering the exothermic heat of WGSR at the intercooler thereafter. The amount of the IP steam produced in situ is more than enough to provide the additional shift steam required for sour shift. As shown in Figure 3, the IP steam is split into three streams. The second steam is sent to the gasifier at a fixed flowrate and the rest is directed to the ~~heat recovery steam generator (~~HRSG~~)~~ for power generation.

After the syngas is shifted, then it is cooled down to 35 °C at which the dual-stage Selexol process (DS Selexol) operates. In both sour and sweet shift cases, the performance targets that the acid gas removal unit has to achieve were set identically as below.

- 90% carbon capture efficiency
- 99.9+% H_2S recovery
- 98.5+% H_2 recovery
- 97+% CO_2 product purity

The Selexol solvent can absorb H_2S more strongly than CO_2 with the selectivity of H_2S over CO_2 around 9 [21]. As shown in Figure 2, firstly the syngas enters the H_2S absorber where its H_2S is absorbed by the CO_2-laden solvent originating from the CO_2 absorber. The H_2S-laden solvent leaving the absorber contains significant amount of CO_2 as well as H_2S. The CO_2 has to be stripped off the solvent before the solvent is regenerated thermally in the ensuing steam stripper. Otherwise, the sour gas would end up with containing vast amount of CO_2 as well as H_2S, making it very hard to achieve the stringent target of the carbon capture efficiency. To this end, removing the CO_2 from the solvent were carried out by a H_2S concentrator (gas stripping) followed by a flash evaporation (depressurisation). By doing so it was possible to direct most of

the CO_2 contained in the solvent to the CO_2 absorber, facilitating such a high carbon capture efficiency.

In the CO_2 absorber, the CO_2 in the feed is selectively absorbed by two solvent streams: one solvent is the lean solvent generated at the steam stripper, containing effectively no CO_2 in it, and the other is the semi-lean solvent originating from the flash drums, less regenerated than the lean solvent. As studied previously by the author [22-24], it is crucial to increase the flowrate of the lean solvent flowrate rather than the semi-lean solvent, if such a high carbon capture efficiency as 95% is targeted (high lean case). But there exists a maximum flowrate that the lean solvent cannot exceed. If too much CO_2-laden solvent was sent to the H_2S absorber, then it would not be possible to recover sufficient CO_2 and return it to the CO_2 cycle. Meanwhile, it is also possible to reach the 90% carbon capture efficiency by increasing the semi-lean solvent, without having to increase the lean solvent (low lean case). In other words, the minimum flowrate of the CO_2-laden solvent required to remove 99.9+% H_2S is found and the stream becomes the lean solvent after being regenerated thermally. In low lean case, the total flowrate of the circulating Selexol solvent would be larger, but it would be easier to return the CO_2 carried by the CO_2-laden solvent to the CO_2 removal section. The total energy consumptions of the two cases were estimated similar to each other.

The net plant efficiency of the IGCC integrated with DS Selexol and sour shift was estimated by process simulation using Honeywell UniSim. As shown in Table 4, the energy penalty incurred by carbon capture integration was around 10.2-% points. The energy penalties at the steam turbine and the auxiliaries were 4.6 and 4.3% points, respectively (Table 5). It should be noted that the increase of the power consumption at the auxiliaries were mainly due to addition of CO_2 capture and compression. The reduction in the steam turbine power generation by carbon capture integration was mainly due to great difference of the amounts of HP steam generated at the syngas cooling stage immediately after the gasifier. In the sour shift case, it is crucial to have the raw syngas contain a vast amount of steam, so that the ensuing sour shift reactors do not require additional shift steam much. To this end, quenching the raw syngas by adding the water is followed by the syngas cooler and the syngas scrubber operating deliberately at a high temperature (200 °C), compared to 110 °C in the non-capture case. The higher temperature does the syngas scrubber operate at, the more steam the syngas can contain [25]. After the syngas quenching, the syngas temperature falls down to 408 °C, so the

amount of the HP steam to be generated by syngas cooler is very limited.

Table 4. Plant performances of decarbonised IGCCs and their comparison with the reference studies.

		Non capture (DOE case 5 [5])	Sour shift (DOE case 6 [5])	Sour shift (This study)	Sweet shift (This study)
Thermal input, MW (HHV)		1547.5	1617.8	1617.8	1617.8
WGSR CO conversion		-	95.6%	95.5%	95.5%
H_2 recovery at DS Selexol		Not reported	Not reported	98.8%	98.5%
H_2S recovery		99.5%	99.7%	99.9+%	99.9+%
CO_2 capture efficiency at the CO_2 absorber		-	Not reported	96.7%	96.2%
Overall carbon capture rate		-	90.0%	89.9%	90.0%
Steam-to-CO ratio		-	2.00	2.03	2.16
Power					
ST power, MW	HP turbine	-	-	44.5	61.2
	IP turbine	-	-	73.6	64.1
	LP turbine	-	-	104.9	94.7
	Total	284.0	229.9	222.9	220.0
GT power, MW		464.0	464.0	464.0	464.0
Total power generation, MW		748.0	693.9	686.9	684.0
AGR auxiliaries, MW		-	15.5	21.6	18.6
Other auxiliary		112.2	132.9	132.8	132.1
CO_2 Compression, MW		-	28.1	32.9	34.4
Total auxiliary power, MW		112.2	176.4	187.4	185.1
Net power, MW		635.8	517.1	499.5	500.9
Net plant efficiency		41.1%	32.0%	30.9%	31.0%

Table 5. Plant performances of decarbonised IGCCs based on sour and shift in this study.

Plant performance	**Non-capture case (DOE case 5, [5])**	**Sweet shift**			**Sour shift**		
		~~Perfromance~~ Performance	Energy change	Energy penalty	~~Performance~~	Energy change	Energy penalty
Thermal input, MW	1547.5	1617.8	70.3	-	1617.8	70.3	-
Gas turbine power	464.0	464.0	0.0	1.30%	464.0	0.0	1.30%
Steam turbine power	284.0	222.0	-62.0	4.63%	222.9	-61.1	4.57%
Total auxiliaries	112.2	185.1	72.9	4.20%	187.4	75.3	4.34%
Net power	635.8	500.9	-136.9	10.10%	499.5	-136.3	10.20%
Net power plant efficiency (HHV)	41.1%	31.0%	-	-	30.9%	-	-

2.2. Sweet Shift Case

In this case, sweet catalysts replaced the sour catalysts, which requires rearrangement of the DS Selexol unit and shift reactors so that shift reactors are to be placed in between desulphurisation and CO_2 removal as shown in Figure 4. However, this seemingly simple change also requires other units to be modified.

It should be noted that, in sweet shift case, the raw syngas does not have to contain vast steam nor maintained hot after the syngas scrubber [25], as this syngas will be sent to the low-temperature H_2S absorber in prior to shift reactors. The syngas does have to contain some water for COS hydrolysis, but the required amount of steam must be very small taking into account the tiny amount of COS in it. In this respect, quenching is no longer needed and the process configuration around the gasifier reverts to what was originally designed for the non-capture case in which it was aimed to generate as much HP steam as possible by heat recovery. The syngas cooling section consists of two heat exchangers for HP steam generation followed by IP BFW heating as is in the sour shift case. The heat duty available in the syngas cooling was distributed between the two heat exchangers by estimating the heat duty at the IP BFW preheater first. The flowrate of the IP BFW to be preheated can be determined by the amount of heat available at the intercooler of the shift reactors in which the IP BFW is to be boiled.

After syngas scrubbing, the syngas is slightly heated by hot HP BFW and then fed to COS hydrolysis in the same way as the syngas is processed in the non-capture case. Then the syngas is cooled down to 35 °C at which the H_2S absorber operates. In the H_2S absorber, the H_2S of the syngas is absorbed selectively by the Selexol solvent originating from the CO_2 absorber. However, the syngas in sweet shift case is very different from that in sour shift case with respect to the composition. In sour shift case, the syngas contains a great amount of CO_2 (45 vol.%) as a result of shift reaction. On the contrary, the syngas in the sweet shift case contains a relatively low amount of CO_2 (3 vol.%). Accordingly, when the CO_2-deficient syngas contacts the CO_2-laden solvent in the H_2S absorber, the CO_2 dissolved in the solvent is stripped off by the syngas. In other words, the H_2S absorber works to absorb the H_2S from the syngas and at the same time strip the CO_2 off the solvent, transferring significant amount of CO_2 from the solvent to the syngas. In turn, it is possible to restrict the CO_2 slip into the sour gas, without having to have a separate H_2S concentrator. Hence, the sweet shift case does not have a H_2S concentrator as shown in Figure 4.

However, the augmented amount of CO_2 in the syngas stream after H_2S removal affects adversely the ensuing shift reaction with respect to the reaction equilibrium. After the gas feed picks up CO_2 upstream of the WGSR, it becomes harder to achieve the targeted CO conversion rate. The greater amount of CO_2 the syngas contains, the more shift steam has to be added to achieve the targeted CO conversion rate. In addition, the syngas leaving the H_2S absorber is still at low temperature, containing much less water vapour than the syngas feed flowing into the sour shift reactor in which it contains significant amount of steam as shown in Table 1.

The amount of CO_2 being transferred from the CO_2-laden solvent to the syngas in the H_2S absorber is highly affected by the flowrate of the CO_2-laden solvent to the H_2S absorber. Increasing the solvent flowrate around the H_2S cycle would make it easier to achieve a very high CO_2 capture rate, as the pinch point is to be formed around the top of the CO_2 absorber to which the CO_2-free Selexol is admitted [24].

The targeted carbon capture efficiency of 90% could be achieved by changing the ratio of the flowrate of the CO_2-free solvent originating from the steam stripper to the flowrate of the semi-lean solvent from the flash drums. As explained above, increasing the CO_2-free solvent flowrate would facilitate reaching the 90% of carbon capture efficiency, as the solvent admitted to the absorber on the top is capable of absorbing CO_2 more strongly than the semi-lean solvent entering the column in the middle. To do so, the flowrate of the CO_2-laden solvent flowing from the CO_2 absorber to the H_2S absorber has to be increased. In turn, it is inevitable to see the syngas pick up more CO_2 from the solvent in the H_2S absorber with the increasing CO_2-laden solvent flowrate. More shift steam would have to be added to the syngas to achieve the targeted CO conversion rate. As discussed in [26], WGSRs often accounts for the largest energy penalty in integrating IGCC with carbon capture. In this respect, it is crucial to maintain the usage of shift steam as low as possible in order to bring down the energy penalty in overall. As a result, low lean case was chosen so as to minimise the flowrate of the CO_2-laden solvent to the H_2S absorber (low lean case).

Assuming the same equilibrium constant of 31 at the outlet of the LT shift reactor, it is also possible to estimate the steam flowrate required to achieve the same 95.5% CO conversion rate by mass balance. When leaving the H_2S absorber, the syngas contains negligible amount of water vapour at 0.0008 kmol/s, while the

required total steam flowrate amounts to 6.5 kmol/s, 0.4 kmol/s greater than the flowrate in sour shift case due to the sweet syngas containing more CO_2 than the syngas in the sour shift case. Therefore, a vast amount of steam has to be added to the syngas.

To source the shift steam, several changes were made to the sour shift case. In sour shift case, the IP steam generated by heat recovery at the intercooler between two shift reactors is split into three sub-streams as shown in Figure 3. The first two streams are used as the diluent of the gasifier and the shift stream. And the rest of it is sent to the HRSG where it is superheated for power generation. In sweet shift case, the portion of the shift steam has to be maximised to compensate the greater demand for shift steam, indicating that no steam is available for power generation any more (Figure 5).

But the increment of the shift steam flowrate is still not large enough for the targeted CO conversion rate. Therefore, another source of shift steam had to be found in the steam cycle. In this study, the additional shift steam was extracted from the HP turbine exhaust. To this end the back pressure of the HP turbine had to be increased up to 38.0 bar from 31.1 bar as the syngas feed has to enter the HT shift reactor at 37.6 bar. The pressure change made to the HP turbine results in significant reduction in the power generation at the HP turbine.

Once shifted, the hot syngas leaving the low temperature shift reactor is cooled down to 35 °C to feed it to the CO_2 absorber. At the same time, the heat is recovered to preheat the WGS feed gas and quenching water and also generate LP steam. It is noticeable that the syngas after sweet shift contains more CO_2 (3.39 kmol/s) and steam (3.63 kmol/s) than the syngas in sour shift case does (3.00 kmol/s CO_2 and 3.26 kmol/s steam), resulting in the total syngas flowrate being larger in sweet shift case (12.0 kmol/s) than in sour shift case (11.3 kmol/s). This is because the syngas feed to shift reaction contains more CO_2 in sweet shift case (0.494 kmol/s) than in sour shift case (0.112 kmol/s) on the grounds of some CO_2 being added to the syngas in the H_2S absorber in the sweet shift case, and accordingly more excess steam has to be added to the syngas for achieving the CO conversion rate. As the shifted syngas has a greater flowrate in sweet shift case, carrying greater heat, its heat recovery can generate more LP steam.

The cold shifted syngas after heat recovery is returned to the DS Selexol unit for carbon capture. Once

processed in DS Selexol unit, the treated syngas stream entering the gas cycle are almost identical in both shift cases in terms of the flowrate and gas composition, indicating that the power generation at the gas cycle would also be identical.

However, the power generation at steam cycle could not but differ significantly between the two cases. Compared to the sour shift case, the sweet shift case has to undergo the following alternations to its steam cycle. The alterations resulting in reduction of the power generation are:

- Reduction of the back pressure of the HP turbine.
- Extraction of the HP turbine exhaust for shift reaction.
- Directing the IP steam generated by recovering the exothermic shift heat to the WGSR instead of the steam cycle.

On the contrary, the changes leading to increase of the power generation are:

- Generating a far greater amount of HP steam at the syngas cooling stage, as quenching is not needed.
- The amount of LP steam generated by cooling the shifted syngas increases, as the syngas is at a higher flowrate, containing more CO_2 and steam.
- Extraction of part of the HP turbine exhaust for shift steam results in less reheat duty in HRSG. Accordingly the HP BFW flowrate admitted to the HRSG is to be increased.

In overall, the amounts of power generation in both sour and sweet shift cases are almost equal, while the power generations at individual steam turbines are very different from each other. The differences between the two shift cases can be explained qualitatively as follows.

- The sweet shift case can generate the HP steam far greater than the sour shift case, resulting in greater power generation at HP turbine. The positive effect of more HP steam generated at syngas cooling outweighs the negative effect of the back pressure of the HP turbine increasing.
- The shift reactors of the sweet shift case ~~requires~~require a far greater amount of additional IP steam.

Accordingly, the power generation at the IP turbine is reduced significantly due to a huge amount of IP steam being extracted from the steam cycle.

- The difference of the power generations at the LP turbine in two shift cases is similar to that at the IP turbine, in spite of the amount of LP steam generated by cooling the shifted syngas being slightly greater in sweet shift case. This is because the LP steam from shifted syngas cooling is of lower quality than the HRSG LP steam with respect to the temperature.

3. Water Gas Shift Reactors

In this section, it was aimed to estimate roughly the size of the two shift reactors in each shift case based on the reaction rate models reported in open literatures. The syngas undergoes water gas shift reaction at two reactors in series: a high temperature shift reactor (HTSR) followed by a low temperature shift reactor (LTSR). The HTSR converts bulk CO to CO_2, while the LTSR can reduce the CO content less than 2 vol.% on dry gas basis.

In the shift reactors, there are several side reactions other than the main reaction taking place at the same time, such as COS hydrolysis, Fischer-Tropsch synthesis, methanol synthesis, etc. But these minor reactions were disregarded in this study, assuming that incorporating these reactions into the reactor models would not affect much the estimation of the reactor size.

All the shift reactors were simulated by a Plug Flow Reactor (PFR) module available in Honeywell UniSim that allows to simulate various heterogeneous catalytic reaction rate models. The overall CO conversion rates in the two shift cases were identical around 95.6%. Due to the high moisture content in the syngas leaving the scrubber, the sour shift needs less steam-to-CO ratio than the syngas in sweet shift case. It was estimated that the ratio of steam to CO was 2.16 in sweet shift and 2.03 in sour shift.

3.1. Sweet Shift

Fe- and Cu-based catalysts were taken for HTSR and LTSR, respectively. As for the high-temperature shift catalyst, the reaction rates were estimated by a power-law rate model [27]. In the Hla et al.'s study [27], two different Fe-based shift catalysts (HTC1 and HTC2), differing with respect to its constituent compositions, were tested and the reaction kinetic models were constructed based on the experimental data. As a result, HTC1 was chosen in this study on the grounds that HTC1 would perform better than HTC2 for a feed gas containing high CO and low CO_2 and H_2, as with the syngas in this study.

Hla et al. [27] proposed the parameter values of the power-law model by testing the HTC1 (80-90 wt% Fe_2O_3/8-13 wt% Cr_2O_3/1-2 wt% CuO) with sulphur-free syngas at 360 – 450 °C and 101.32 kPa.

$$r_{HTC1}\left(\frac{mol}{g_{cat}\,s}\right) = 10^{2.845}\left(\frac{mol}{g_{cat}\,s\,kPa^{0.55}}\right) e^{\frac{-111000\left(\frac{J}{mol}\right)}{RT}} P_{CO} P_{CO_2}^{-0.36} P_{H_2}^{-0.09}\left(1 - \frac{1}{K_e}\frac{P_{CO_2}P_{H_2}}{P_{CO}P_{H_2O}}\right) \quad (2)$$

where P_tP is partial pressure [kPa].

The raw syngas undergoes the CO conversion rate of around 79% in the HTSR. The hot syngas leaving the HTSR is cooled by boiling hot IP BFW and then it is fed successively to the ensuing LTSR for reducing the CO mole fraction further.

As can be seen in the reaction kinetic model of the HTC1, the activation energy of the rate constant is as high as -111 kJ/mol, indicating that the reaction rate would be very low in the temperature range of the LTSR, 270 – 317 °C. In this relatively low temperature range of the LTSR, the Fe-based HTS catalyst would end up with a very low reaction rate.

Hence a Cu-based catalyst, exhibiting a very high reaction rate in the low temperature, has to be chosen instead. In this study, it was assumed that the LTSR was packed with a commercial $CuO/ZnO/Al_2O_3$ (50/40/10 wt%) catalyst referred to LTS. Mendes et al. [28] proposed a Langmuir-Hinshelwood model along with its associated parameter values by testing the Cu-based catalyst with sulphur-free syngas in the range of 180 – 300 °C and at 101.32 kPa as follows [28].

$$r_{LTS}\left(\frac{mol}{g_{cat}\,s}\right)=\frac{6.153\,10^{-8}\left(\frac{mol}{g_{cat}\,s\,Pa^{2}}\right)e^{-\frac{3783\left(\frac{J}{mol}\right)}{RT}}P_{CO}P_{H_2O}\left(1-\frac{1}{K_e}\frac{P_{CO_2}P_{H_2}}{P_{CO}P_{H_2O}}\right)}{\left(1+1.756\times10^{-27}e^{\frac{80410}{RT}}P_{CO}+9.321\times10^{-4}e^{\frac{4109}{RT}}P_{H_2O}+2.28\times10^{-3}e^{\frac{9795}{RT}}P_{CO_2}+2.739\times10^{-12}e^{\frac{83608}{RT}}P_{H_2}\right)^{2}} \quad (3)$$

$$r_{LTS}=\frac{6.153\times10^{-14}e^{-\frac{3783}{RT}}P_{CO}P_{H_2O}\left(1-\frac{1}{K_e}\frac{P_{CO_2}P_{H_2}}{P_{CO}P_{H_2O}}\right)}{\left(1+1.756\times10^{-30}e^{\frac{80410}{RT}}P_{CO}+9.321\times10^{-7}e^{\frac{4109}{RT}}P_{H_2O}+2.28\times10^{-6}e^{\frac{9795}{RT}}P_{CO_2}+2.739\times10^{-15}e^{\frac{83608}{RT}}P_{H_2}\right)^{2}} \quad (3)$$

Formatted

where P_tP is partial pressure [Pa].

According to Eq.3, the Cu-based catalyst would have a reaction rate greater than the Fe-based catalyst, even at the operation conditions of the HTSR. However, the Cu-based catalyst had to be employed for a shift reactor operating in the relatively low temperatures, as it would be easily deactivated by thermal sintering in the HTSR temperature [29].

In estimating the reaction rates at the IGCC pressure as high as 35 bar, it may be presumptuous to make use of the reaction rate models constructed by testing the catalysts at ambient pressure. In this respect, Eq. 4 was taken as a pressure correction factor and is applied to each reaction rate model, similarly to the earlier works [30, 31].

$$P_t = P^{0.5-P/500} \quad (4)$$

where P is actual system pressure [atm]. The pressure correction factor is known to be valid up to 55 atm [32, 33].

3.2. Sour Shift

It is not recommended to use the sweet shift catalysts presented above for a syngas feed containing a high concentration of hydrogen sulphide, as the Fe or Cu based catalysts would exhibit significant reduction in the reaction rates as well as lose the catalytic activity greatly when exposed to H_2S [27].

As for the sour shift, a Co-Mo based catalyst ($CoO/MoO_3/MgO/Al_2O_3$/promoter = 2:8:24:50:balance wt%), referred to SSC, was chosen, as this catalyst's activity could be promoted by the sulphur compounds

contained in a syngas feed. Hla et al. [34] carried out experiments to measure the shift reaction rates of gases containing 1000 H_2S ppmvw on SSC in the range of 350 – 450 °C and at 101.32 kPa. They proposed that the reaction rate could be estimated by a power-law model as follows [34]:

$$r_{SSC,1000ppmv\ H_2S}\left(\frac{mol}{g_{cat}\ s}\right) = 0.008\left(\frac{mol}{g_{cat}\ s\ kPa^{0.9}}\right) e^{\frac{-60300\left(\frac{J}{mol}\right)}{RT}} P_{CO}^{0.75} P_{H_2O}^{0.31} P_{CO_2}^{-0.07} P_{H_2}^{-0.09} \left(1 - \frac{1}{K_e}\frac{P_{CO_2}P_{H_2}}{P_{CO}P_{H_2O}}\right) \quad (5)$$

Hla et al. [34] also investigated the effect of H_2S on the shift reaction rates with the H_2S concentration in the feed gas varied from 330 to 2670 ppmwppmv. When plotted in log-log graph, the experimental data exhibited linearity. Accordingly, the effect of H_2S on the reaction rate is expressed by

$$r_{SSC}\left(\frac{mol}{g_{cat}\ s}\right) = r_{SSC,1000ppmv\ H_2S}\left(\frac{mol}{g_{cat}\ s}\right)\left[\frac{H_2S\ ppmwv}{1000}\right]^n \quad (6)$$

where n is the slope of the trend line in the logarithmic coordinate, estimated 0.52 in their experimental study [34]. Similarly to the study on the sweet shift catalysts, the pressure correction factor, Eq. 4, was applied to the reaction rate models, in order to estimate the reaction rates at the very high pressure from those estimated at ambient pressure for sizing the high-pressure reactor. It was assumed that the SSC catalysts be applicable to both HTSR and LTSR in sour shift case.

For simplicity, it was assumed that all three catalysts had identical particle density (2400 kg/m^3) and bulk density (1200 kg/m^3). Also the following assumptions were made: no pressure drop, adiabatic reactors, plug flow, no radial distributions of temperature and concentration, negligible mass transfer resistances at the film and in the pore and no axial dispersion.

3.3. Comparison of the Sweet and Sour Shift Reactors

With the assumptions made above, a reactor size is to be estimated only by a plug flow reactor model including the shift reaction rate model. First, the chosen rate models were tested to see if they could replicate the experimental results reported in the references. Hla et al. [27] measured the CO conversion rate at 450 °C

and 1 atm when a dry-feed coal-derived syngas was fed to a lab-scale reactor packed with HTC1 in the conditions of the actual gas space velocity of 1.9 m^3 $gcat^{-1}$ h^{-1} and the steam-to-carbon ratio of around 3. The experimental CO conversion was reported around 7.8%, while its equivalent simulation of this study resulted in 5.6% CO conversion assuming isothermal operation.

Hla et al. [34] tested the SSC1 catalyst with a dry-feed coal-derived syngas containing 1000 ~~ppmw~~ ppmv H_2S at 450 °C and 1 atm with the steam-to-carbon ratio adjusted to 3. The experimental CO conversion rate was around 1.5 mol $gcat^{-1}$ s^{-1}, while its value estimated by UniSim PFR was 1.1 mol $gcat^{-1}$ s^{-1}.

As for the Cu-based catalyst, Mendes et al. [28] reported the CO conversion rates when a typical reformate gas was fed to a lab-scale reactor at 1.2 bar with both the reaction temperature and the contact time varied. Again, the experimental results were compared with the simulation results by solving the reaction rate model applicable to a broader temperature range, 180 – 300 °C, with UniSim PFR. The PFR simulation results were slightly lower than the experimental CO conversion rates, as the differences between the two were within 6% points in most data. For example, the UniSim PFR estimated the CO conversion rate of 44%, while the experimental value was 48%, at the contact time of 12.9 gcat h mol^{-1} and 200 °C.

In those papers proposing the reaction rate equations, each parameter was reported as an average value that is allowed to vary in a range. By adjusting the parameters within their associated ranges, it might be possible to make the simulation results closer to the experimental results. In this study, however, such laborious works were not attempted on the grounds that when the reaction rate models were implemented with the average parameter values, they could reproduce the experimental results reasonably well. Again this part of study was aimed to estimate roughly the amount of shift catalysts required to achieve the desired CO conversion rate in the sweet and sour shift cases.

In this study, the length of a shift reactor was determined so that the CO conversion rate could reach 99% of the equilibrium conversion for all four reactors with the diameter set as 3.5 meter. Table 6 summarises the simulation results of all four shift reactors. As for the high temperature shift reactors, the lengths of the two reactors were relatively close to each other. The sweet shift reactor was 8.8 meter and the sour shift reactor was 5.9 meter. As explained above, it is essential to incorporate the H_2S correction factor, Eq. 6, into the

reaction rate equation in sour shift case, as the reaction rate would be promoted greatly by the presence of H_2S in the feed. Otherwise, the CO conversion rate plunged to 34% from 77% in the same reactor.

However, the reactor lengths required for low temperature shift reaction were very different between the two shift cases. The reactor packed with the Cu-based catalysts for sweet shift was estimated only 6.3 meters long, but the sour shift reactor with the CoMo-based catalysts had to be 64 meter long. This is due to the reaction rate model found for the sour shift catalyst predicting very low reaction rates in the temperature range of the LTSR as shown in Table 6. This puzzling result indicates that the chosen CoMo catalysts would be effective only in the temperature ranges well above the LTSR temperature [35] and other sulphur-resistant catalysts must be taken for the LTSR. To the best of our knowledge, such catalysts are commercially available, but their reaction rate models have not been reported in open literatures yet.

Table 6. Size of the shift reactors estimated by the reaction rate models at the condition of 99% approach to the equilibrium CO conversion.

	Sweet HTSR	Sweet LTSR	Sour HTSR	Sour LTSR
Catalyst	**HTC1 (Fe-based catalyst)**	**LTS (Cu-based catalyst)**	**SSC (CoMo-based catalyst)**	**SSC (CoMo-based catalyst)**
Volume, m^3	84.7	60.6	56.8	615.8
~~Diameter, m~~	~~3.5 m~~	~~3.5 m~~	~~3.5 m~~	~~3.5 m~~
~~Length, m~~	~~8.8 m~~	~~6.3 m~~	~~5.9 m~~	~~64 m~~
CO conversion rate	77.9%	78.4%	77.1%	78.5%
Average reaction rate [mol/cm^3/s]	$2.78 \cdot 10^{-5}$	$8.63 \cdot 10^{-6}$	$4.11 \cdot 10^{-5}$	$8.83 \cdot 10^{-7}$

4. Conclusions

In this study, the two process configurations of an IGCC integrated with either sour or sweet shift catalytic reactors were designed, to see which alterations had to be made to syngas cooling, shift reactors, acid gas removal unit and steam cycle. Based on the detailed process flowsheets, the energy penalty incurred by carbon capture integration was estimated more accurately than ever. As expected, the sweet shift case would require a far greater amount of additional shift steam than the sour shift case. Contrary to the stereotype of sweet shift resulting in a greater energy penalty than sour shift, however, the energy penalties incurred by carbon capture integration were almost equal in both shift cases. This was mainly due to the sweet shift case not requiring syngas quenching. Note that if the sweet shift case would be configured in the same way as the sour shift case up to the syngas scrubber, including water quenching and operating the syngas scrubber at the higher temperature, the sweet shift case would incur 3.7 % points greater energy penalty than the sour shift case.

The CO_2 absorber of the DS Selexol process runs with two solvents: lean solvent and semi-lean solvent. The two solvent flowrates are complementary to each other, i.e. increasing the lean solvent flowrate allows to reduce the semi-lean flowrate or vice versa. Accordingly, the DS Selexol process could be designed in two different modes: high lean or low lean modes. In the sweet shift case, however, the low lean mode has to be chosen, as the amount of CO_2 transferred to the syngas from the solvent taking place at the H_2S absorber must be minimised. Otherwise, the syngas leaving the H_2S absorber would contain more CO_2, requiring more shift stream to be added for the ensuing shift reactors. With respect to the process configuration, the sweet

Formatted: Font: (Default) Times New Roman, 8 pt, Font color: Black

Formatted: Left, None, Space Before: 0 pt, After: 0 pt, Line spacing: single, Don't keep with next, Don't keep lines together, Adjust space between Latin and Asian text, Adjust space between Asian text and numbers

Formatted Table

Formatted: Font: (Default) Times New Roman, 8 pt, Bold, Font color: Black

Formatted: Left, Space After: 0 pt, Line spacing: single, Adjust space between Latin and Asian text, Adjust space between Asian text and numbers

Formatted: Font: Not Bold

Formatted: Font: (Default) Times New Roman, 8 pt, Font color: Black

Formatted: Left, Space After: 0 pt, Line spacing: single, Adjust space between Latin and Asian text, Adjust space between Asian text and numbers

Formatted Table

Formatted: Font: (Default) Times New Roman, 8 pt, Font color: Black

Formatted: Font: (Default) Times New Roman, 8 pt, Font color: Black

Formatted

Formatted

Formatted

Formatted

Formatted

Formatted

Formatted

Formatted

Formatted

Formatted

Formatted

shift case does not need to have a H_2S concentrator separately, as the H_2S absorber also functions as enriching H_2S in the H_2S-laden solvent by stripping CO_2 off the solvent.

In sizing the shift reactors with the reaction rate models found in the literatures, it was found that the sizes of the high-temperature shift reactors are comparable to each other. However, the low temperature sour shift reactor had to be sized much larger than the equivalent sweet shift reactor, due to the sour shift catalysts exhibiting one order of magnitude lower reaction rates than the sweet catalysts in the operating conditions of the catalytic reactor. However, all the reactor sizing of this study may need to be updated afterwards, once the latest shift catalysts are experimented and their reaction rate models are found and reported. In this study, the CoMo catalyst performing excellently at high temperatures were also taken for the low temperature shift reactor of the sour shift case, as to the best of our knowledge any other catalysts suitable for this reactor had not been proposed with the reaction rate model as yet.

Acknowledgements

Financial support from EPSRC grant (EP/N024672/1) is gratefully acknowledged.

References

[1] Demirbas A. Potential applications of renewable energy sources, biomass combustion problems in boiler power systems and combustion related environmental issues[Progress in Energy and Combustion Science. 2005;31(2):171-92.

[2] Shafiee S, Topal E. When will fossil fuel reserves be diminished? Energy Policy. 2009;37(1):181-9.

[3] Müller S, Brown A, Ölz S. Renewable energy: Policy considerations for deploying renewables. Paris, France: International Energy Agency. 2011.

[4] Olah GA. Beyond oil and gas: the methanol economy. Angew Chem Int Ed Engl. 2005;44(18):2636-9.

[5] DOE/NETL. Cost and performance baseline for fossil energy plants. Volume 1: Bituminous coal and natural gas to electricity final report. National Energy Technology Laboratory. 2007.

[6] DOE/NETL. Cost and performance baseline for fossil energy plants volume 1: bituminous coal and natural gas to electricity Revision 2. 2010.

[7] Black J. Cost and performance baseline for fossil energy plants volume 1: bituminous coal and natural gas to electricity. National Energy Technology Laboratory: Washington, DC, USA. 2010.

[8] Guardian T. No new coal without catbon capture, UK government rules. 2009.

[9] Blomen E, Hendriks C, Neele F. Capture technologies: Improvements and promising developments. Enrgy Proced. 2009;1(1):1505 - 12.

[10] NETL D. Water gas shift & hydrogen production.

[11] Descamps C, Bouallou C, Kanniche M. Efficiency of an Integrated Gasification Combined Cycle (IGCC) power plant including CO2 removal. Energy. 2008;33(6):874-81.

[12] Hallmark B, Parra-Garrido J, Murdoch A, Salmon I, Hodrien C. Benchmarking the Timmins Process - a novel approach for low energy pre-combustion carbon capture in IGCC flowsheets. Canadian Journal of Chemical Engineering. 2017;95(6):1023-33.

[13] Sheikh HM, Ullah A, Hong K, Zaman M. Thermo-economic analysis of integrated gasification combined cycle (IGCC) power plant with carbon capture. Chemical Engineering and Processing. 2018;128:53-62.

[14] Trapp C, Thomaser T, van Dijk HAJ, Colonna P. Design optimization of a pre-combustion CO2 capture plant embedding experimental knowledge. Fuel. 2015;157:126-39.

[15] Kanniche M, Bouallou C. CO2 capture study in advanced integrated gasification combined cycle. Applied Thermal Engineering. 2007;27(16):2693-702.

[16] Huang Y, Rezvani S, McIlveen-Wright D, Minchener A, Hewitt N. Techno-economic study of CO2 capture and storage in coal fired oxygen fed entrained flow IGCC power plants. Fuel Processing

Technology. 2008;89(9):916-25.
[17] Cormos CC, Cormos AM, Agachi S. Power generation from coal and biomass based on integrated gasification combined cycle concept with pre- and post-combustion carbon capture methods. Asia-Pacific Journal of Chemical Engineering. 2009;4(6):870-7.
[18] Cormos C-C, Agachi PS. Integrated assessment of carbon capture and storage technologies in coal-based power generation using CAPE tools. Computer Aided Chemical Engineering: Elsevier; 2012. p. 56-60.
[19] Padurean A, Cormos CC, Agachi PS. Pre-combustion carbon dioxide capture by gas-liquid absorption for Integrated Gasification Combined Cycle power plants. International Journal of Greenhouse Gas Control. 2012;7:1-11.
[20] Prins M, Van den Berg R, Van Holthoon E, Van Dorst E, Geuzebroek F. Technological Developments in IGCC for Carbon Capture. Chemical Engineering & Technology. 2012;35(3):413-9.
[21] Bucklin RW, Shendel, R.L. Comparison of fluor solvent and Selexol processes. Energy Progress. 1984;4:137-42.
[22] Ahn H. Process Simulation of a Dual-stage Selexol Process for Pre-combustion Carbon Capture at an Integrated Gasification Combined Cycle Power Plant. Process Systems and Materials for CO2 Capture: Modelling, Design, Control and Integration. 2017:609-28.
[23] Ahn H, Kapetaki Z, Brandani P, Brandani S. Process simulation of a dual-stage Selexol unit for pre-combustion carbon capture at an IGCC power plant. Enrgy Proced. 2014;63:1751-5.
[24] Kapetaki Z, Brandani P, Brandani S, Ahn H. Process simulation of a dual-stage Selexol process for 95% carbon capture efficiency at an integrated gasification combined cycle power plant. International Journal of Greenhouse Gas Control. 2015;39:17-26.
[25] Kapetaki Z, Ahn H, Brandani S. Detailed process simulation of pre-combustion IGCC plants using coal-slurry and dry coal gasifiers. Enrgy Proced. 2013;37:2196-203.
[26] Beavis R, Forsyth J, Roberts E, Song B, Combes G, Abbott J, et al. A Step-change Sour Shift process for improving the efficiency of IGCC with CCS. Enrgy Proced. 2013;37:2256-64.
[27] Hla SS, Park D, Duffy GJ, Edwards JH, Roberts DG, Ilyushechkin A, et al. Kinetics of high-temperature water-gas shift reaction over two iron-based commercial catalysts using simulated coal-derived syngases. Chemical Engineering Journal. 2009;146(1):148-54.
[28] Mendes D, Chibante V, Mendes A, Madeira LM. Determination of the Low-Temperature Water-Gas Shift Reaction Kinetics Using a Cu-Based Catalyst. Industrial & Engineering Chemistry Research. 2010;49(22):11269-79.
[29] Twigg MV, Spencer MS. Deactivation of supported copper metal catalysts for hydrogenation reactions. Applied Catalysis a-General. 2001;212(1-2):161-74.
[30] Singh CPP, Saraf DN. Simulation of High-Temperature Water-Gas Shift Reactors. Industrial & Engineering Chemistry Process Design and Development. 1977;16(3):313-9.
[31] Singh CPP, Saraf DN. Simulation of Low-Temperature Water-Gas Shift Reactor. Industrial & Engineering Chemistry Process Design and Development. 1980;19(3):393-6.
[32] Adams II TA, Barton PI. A dynamic two-dimensional heterogeneous model for water gas shift

reactors. International Journal of Hydrogen Energy. 2009;34(21):8877-91.
[33] Mobed P, Maddala J, Rengaswamy R, Bhattacharyya D, Turton R. Data Reconciliation and Dynamic Modeling of a Sour Water Gas Shift Reactor. Industrial & Engineering Chemistry Research. 2014;53(51):19855-69.
[34] Hla SS, Duffy GJ, Morpeth LD, Cousins A, Roberts DG, Edwards JH. Investigation into the performance of a Co-Mo based sour shift catalyst using simulated coal-derived syngases. International Journal of Hydrogen Energy. 2011;36(11):6638-45.
[35] Plaza A, Fail S, Cortes JA, Fottinger K, Diaz N, Rauch R, et al. Apparent kinetics of the catalyzed water-gas shift reaction in synthetic wood gas. Chemical Engineering Journal. 2016;301:222-8.